https://doi.org/10.5194/egusphere-2025-5666
Preprint. Discussion started: 20 November 2025

Spectral Analysis of Groundwater Level Time Series for Robust Estimation of Aquifer Response Times

Timo Houben[1,4], Christian Siebert[2], Thomas Kalbacher[3], Mariaines Di Dato[1], Thomas Fischer[3], and Sabine Attinger[1,4]

[1]Department of Computational Hydrosystems, Helmholtz Centre for Environmental Research - UFZ, Leipzig, Germany
[2]Department Catchment Hydrology, Helmholtz Centre for Environmental Research - UFZ, Theodor-Lieser-Str. 4, 06120 Halle, Germany
[3]Department of Environmental Informatics, Helmholtz Centre for Environmental Research - UFZ, Leipzig, Germany
[4]Institute of Environmental Science and Geography, University of Potsdam, Karl-Liebknecht-Str. 24-25, 14476 Potsdam, Germany

Correspondence: Timo Houben (timo.houben@ufz.de)

Abstract. Groundwater resources represent Germany's most important source of freshwater but they are increasingly under pressure. Climate change, societal developments, and rising abstraction rates are impacting subsurface storage in ways that are currently difficult to predict, affecting both the quantity and quality of groundwater. To ensure sustainable groundwater management, it is crucial to evaluate the intrinsic and spatially variable vulnerability of groundwater systems, especially to prepare for the effects of hydrological extremes. In this context, the groundwater response time, defined as the timescale over which a groundwater system responds or adjusts to changes in external or internal conditions, serves as a valuable indicator for vulnerability assessments. Unlike traditional methods, we propose estimating response times through spectral analysis of groundwater level data. Time series from nearly 200 selected observation wells across Bavaria in Southern Germany were processed and transformed into the spectral domain. Corresponding recharge time series were extracted from high-resolution hydrological model outputs. By integrating these data with hydrogeomorphic information, we fitted a semi-analytical model to the groundwater level spectra to obtain aquifer response times. The semi-analytical solution for the spectral domain accurately reproduced the majority of observed groundwater level spectra. Most estimated response times fall between roughly 50 and 300 days. Significant correlation were found between the response time and the depth of the groundwater table. Groundwater systems exhibiting longer response times are interpreted as more resilient to drought conditions and therefore potentially better suited for groundwater abstraction than aquifers with shorter response times.

1 Introduction

In the last decade, Central Europe experienced a series of hot and dry periods resulting in severe droughts such as the extraordinary drought period in 2018-2020. These conditions greatly affected groundwater systems, as increased abstraction for house-

https://doi.org/10.5194/egusphere-2025-5666
Preprint. Discussion started: 20 November 2025

holds, industry, and agriculture set additional pressure on water resources (Wanders and Wada, 2015). Furthermore, during the winter season, droughts were accompanied by reduced groundwater recharge, leading to lower replenishment of groundwater systems compared to normal conditions. Jasechko et al. (2024) analyzed more than 100 000 data sets for more than 1 600 aquifer systems worldwide and showed that rapid groundwater level declines (more than 0.5 m per year) are widespread in the twenty-first century, especially in dry regions with extensive cropland areas. In summary, both reduced recharge and excessive water withdrawals contribute to declining groundwater levels, which in turn leads to a decrease in baseflow that sustains river systems.

Beside evidence from past data analysis, model-based hydrometeorological projections state that the risks of droughts-in particular longer lasting and stronger droughts-will continue to increase in Europe (Ciscar et al., 2019; European Commission, 2021; IPCC, 2023). Coupled climate-hydrological model simulations by Samaniego et al. (2018) project more frequent soil moisture droughts across Europe, along with a 40 % $\pm$ 24 % increase in drought-affected areas, if global warming reaches 3 K. The consequences on groundwater recharge and thus groundwater systems, however, are difficult to estimate and subject of great uncertainty-at least in Central Europe (Kumar et al., 2025).

A central question therefore is: how long are groundwater systems capable of buffering periods of strongly reduced groundwater recharge or strongly increased groundwater withdraws? An essential property describing the capacity of groundwater systems to buffer and moderate fluctuations in recharge or pumping stresses is the groundwater response time (also known as aquifer response time or characteristic time). This parameter quantifies the time required for the groundwater system to relax after or respond to changes in recharge rates or excessive abstraction (Houben et al., 2022; Jazaei, 2017).

Various methods exist to estimate groundwater response times, based on time series of groundwater levels or baseflow. A common approach is to measure the lag time between a specific event such as a drought during which recharge to the system ceases and the response of the groundwater level. The recession time of baseflow under such drought situations or the recovery time of baseflow after the drought has ended is then considered to be the response time of the contributing aquifer systems (Brutsaert, 2008). Lee and Ajami (2023) analyzed data of baseflow data from 358 anthropogenically unaffected catchments across the United States to characterize droughts and recovery properties of baseflow. The catchments they investigated showed baseflow droughts that last between 9–104 months, which is longer than the corresponding precipitation droughts. A challenge in applying this approach is accurately defining the start and end of a dry period, as these depend on the characteristics of each specific event. This might also explain why Hameed et al. (2023) found large variations in recession constants for a single catchment using event-based recession analysis.

Another approach is to consider groundwater systems as systems that continuously receive recharge driven by precipitation and also react to this continuously varying stimulus with fluctuating groundwater levels and temporarily varying baseflow. Within this context, response times are often estimated by correlating standardized groundwater level or baseflow data with standardized time series of precipitation accumulated for different periods. Following this approach, Hellwig and Stahl (2018) investigated past changes and potential future changes in baseflow for 338 headwater catchments across Germany. They presented baseflow response times that vary across Germany, ranging from a few months to several years. In addition, the resulting response times depend on the hydrogeological properties of the catchments. A limitation of using baseflow data, however, is

https://doi.org/10.5194/egusphere-2025-5666
Preprint. Discussion started: 20 November 2025

that it describes the response of aquifer systems at the catchment level. The analogous analysis of groundwater level data allows to infer local groundwater response times. Boumaiza et al. (2021) found aquifer response times between one and three months in Saint-Honoré aquifer in Canada using a sliding cross-correlogram approach and Kumar et al. (2016) analyzed groundwater level data from the Danube and additional catchments in the Netherlands. Both, Kumar et al. (2016) and Boumaiza et al. (2021) observed that response times differ within a given aquifer and are influenced by the thickness of the vadose zone. Thicker vadose zones lead to longer response times. The latter result points to a limitation of this method: the response time estimates include the transit time of the pressure signal through the vadose zone. Therefore, they are not only reflecting the aquifer response times but also the response time of the whole coupled subsurface system.

Several theory-based approaches have evolved over recent decades (Gelhar and Wilson, 1974; Erskine and Papaioannou, 1997; de Rooij, 2012, 2013; Jazaei, 2017; Carr and Simpson, 2018). For example, dimensional analysis of the linearized Boussinesq equation (Bear, 1972; Freeze, 1979) demonstrates that a characteristic time scale of an aquifer is governed by a combination of three key parameters: a typical length L, the storativity S and the transmissivity T of an aquifer which relate as follows:

$$t_c = \frac{L^2 S}{T} \tag{1}$$

Cuthbert et al. (2019) and colleagues applied this formula to estimate groundwater response times on a global scale. They used globally derived values for the relevant parameters and incorporated them into the formula. The result is a gridded map of groundwater response times, which typically range from several years to several hundred years. These results clearly contradicts results of much smaller response times presented by Hellwig and Stahl (2018), Houben et al. (2022) and Kumar et al. (2016) for German catchments, Boumaiza et al. (2021) for Canadian aquifer systems, as well as our findings in this work.

Recently, Carr and Simpson (2018) developed a new method for calculating highly accurate estimates of response times for groundwater flow processes. The analysis is carried out using the linearized, one-dimensional Dupuit-Forchheimer model of saturated flow through a heterogeneous porous medium and is based on hydraulic head (i.e., hydrostatic pressure) measurements.

Alternatively, spectral approaches can be used to infer response times. Zhang and Schilling (2004, 2005); Zhang and Li (2006); Zhang and Yang (2010); Schilling and Zhang (2011); Liang and Zhang (2013, 2015); Zhang et al. (2022); Pujades et al. (2023) investigated the spectral analysis method (SpA) based on semi-analytical solutions of groundwater flow equations for the frequency domain and analyzed various groundwater systems. Houben et al. (2022) demonstrated its capability to estimate aquifer parameters like response times, storativity as well as transmissivities from long groundwater time series in a virtual (numerical) aquifer and exemplarily applied the method to measured data from groundwater levels in central Germany. As an advantage, spectral methods yield response time estimates that reflect the system's overall dynamic behavior, since the full spectrum of frequencies is analyzed. This contrasts with recession constant analysis, which relies on identifying and analyzing individual events. A potential drawback of frequency domain approaches is that sufficiently long time series of groundwater data are required.

https://doi.org/10.5194/egusphere-2025-5666
Preprint. Discussion started: 20 November 2025

In this work, we apply the spectral analysis method (SpA) introduced by Houben et al. (2022) to groundwater level time series from 209 observation wells in Bavaria, Germany. We confirm and further demonstrate the robustness of the approach in determining groundwater response times from real data and provide thorough interpretation of the results.

The Methodology section outlines the theoretical foundations of spectral analysis, detailing a systematic workflow encompassing data preparation, pre-processing, and final parameter estimation. The Results section presents representative types of groundwater level spectra along with the corresponding estimates of aquifer response times. An in-depth Discussion addresses the uncertainties inherent in the analysis and explores the broader implications of the findings. Finally, concluding remarks are presented at the end of this work.

2 Methodology

2.1 Theoretical Background

Aquifers typically act as low-pass filters (Zhang and Schilling, 2004), i.e., they transform incoming signals, such as the recharge, into a signal with decreased (dampened) high frequency content above a specific cut-off frequency. This cut-off frequency is inversely related to the aquifer response time.

Spectral analyses relies on the Fourier transform of a temporal signal $g(t)$ (e.g., measured groundwater levels over time). The Fourier transform is defined by the following equation:

$$\hat{g}(\omega) = \int_{-\infty}^{\infty} g(t)\, e^{2\pi i \omega t} dt \tag{2}$$

where $i = \sqrt{-1}$ and ω is the frequency. $\hat{g}(\omega)$ represents the frequency share of the original signal. The Fourier transform of the temporal autocorrelation function R_{hh} of the signal is the spectral density S_{hh} (in this work also referred to as spectrum)

$$S_{hh}(\omega) = \int_{-\infty}^{\infty} R_{hh}(\tau)\, e^{-2\pi i \omega \tau} d\tau \tag{3}$$

where R_{hh} is assumed to be stationary in time and τ is the time. Based on this relation, Liang and Zhang (2013) developed a semi-analytical solution for a groundwater head spectrum of an 1D groundwater transect with homogeneous aquifer properties. Details of its derivation can be found in Liang and Zhang (2013) and Houben et al. (2022). The final equation reads:

$$S_{hh}(x,\omega) = \frac{16}{\pi^2 S^2} \sum_{m=0}^{\infty} \sum_{n=0}^{\infty} \frac{(-1)^{m+n} B_m B_n S_{ww}}{(2m^2+2n^2+2m+2n+1)} \cdot \frac{(2m+1)^2}{(2m+1)^4 (\frac{4}{pi^2} t_c)^{-2} + \omega^2} \tag{4}$$

$$B_m = \frac{cos[(2m+1)\pi x'/2]}{(2m+1)}, \qquad x' = \frac{x}{L} \tag{5}$$

https://doi.org/10.5194/egusphere-2025-5666
Preprint. Discussion started: 20 November 2025

It relates the spectrum of groundwater level fluctuations S_{hh} at a certain location to the groundwater recharge spectrum S_{ww}. S is the storativity, x is the distance of the observation well (where time series are recorded) to the water divide and L is the aquifer length from the water divide to the river. Then, the response time t_c is given by

$$t_c = \frac{L^2 S}{T} \tag{6}$$

t_c depends on the length L, the storativity S and the transmissivity T of the observed aquifer. It can range from a few weeks for small and highly conductive aquifers with low specific storage to several months or years for large aquifers with low transmissivities and higher storativities.

2.2 Data and Workflow

2.2.1 Study Area: Bavaria

Central for the analysis are long time series of groundwater level measurements at different locations and hydrogeological units. For this study, 298 groundwater observation wells from the monitoring network of the Bavarian State Office for the Environment (LfU) representing the upper groundwater stockwork (groundwater table depth smaller than 100 m) were selected and the corresponding groundwater level time series were downloaded via the online service (Bayerisches Landesamt für Umwelt, 2022). The wells are distributed throughout the state and cover relevant hydrogeological units where groundwater abstraction takes place (Fig. 1a. The State of Bavaria is located in the south of Germany and its southern border is dominated by the up to 3 000 m high Alpine Mountains with steep folded hard rocks with low groundwater yield. Northward the mountains transit into the wide and flat Molasse Basin, which is filled with unconsolidated debris from the Alps, hosting most productive shallow aquifers. Similarly, Quaternary valley fillings constitute productive aquifers. In the center and northern parts of the state however, faulted blocks of Mesozoic lime-, dolo- and sandstones form the hilly landscape and host groundwater in medium productive and partly karstified aquifers. These areas are framed by lifted blocks of crystalline Paleozoic basement forming a few hundreds meters high mountain ranges. No groundwater observations exist there. Even if the time series are distributed all over the hydrogeological units, forming the upper groundwater storey, the majority of observation wells are located in the Molasse Basin and Quaternary sediments surrounding the larger rivers draining from the Alps through glacier valleys towards the Danube River (Fig. 1a).

2.2.2 Time Series Preparation (Fig. 2a and b)

The majority of the groundwater time series cover at least 15-20 years of data with a few being 50 years long. All of them end at the beginning of 2019. Houben et al. (2022) demonstrated that time series should cover a time duration of at least ten times the expected characteristic time of the aquifer to obtain correct estimates of the power spectrum containing all frequencies with enough spectral power. Following this, time series with a length of less than 2 years were discarded. Finally 224 time series remained for the analysis.

https://doi.org/10.5194/egusphere-2025-5666
Preprint. Discussion started: 20 November 2025

First, the raw data was processed to obtain time series suitable for the analysis. In a first step, outliers were removed using the interquartile range $IQR = Q_3 - Q_1$. The lower limit was determined as $lim_{low} = (Q_1 - 1.5 * IQR)$ while the upper limit was defined as $lim_{up} = (Q_3 - 1.75 * IQR)$. In a second step, the time series were interpolated to ensure equidistant time steps of one day. Linear, cubic, polynomial and PCHIP interpolation methods were applied to the time series. PCHIP turned out to be the best performing method since it preserves monotonicity without overshooting and avoids artificial curvatures (Fritsch and Carlson, 1980).

In addition, recharge time series were required. The necessary recharge time series were provided as a gridded dataset generated by the mesoscale Hydrologic Model (mHM) (Marx et al., 2021; Samaniego et al., 2010; Kumar et al., 2013; Zink et al., 2017). The recharge time series from multiple grid cells surrounding the grid cell containing the observation well were extracted and spatially averaged.

The groundwater level and recharge time series were aligned to the same time period, and linear trends were removed. Removing the linear trend prevents artificial low-frequency components from distorting the frequency domain analysis, ensures the data are closer to stationarity, and helps revealing true periodic signals by reducing spectral leakage. It is often applied when dealing with groundwater data in the spectral domain (Jiménez-Martínez et al., 2013, e.g.,). Some exemplary time series of groundwater head time series are depicted in Fig. 1b.

2.2.3 Transformation of time series into frequency domain (Fig. 2a and b)

Power spectra of head and recharge time series were estimated with Welch's method (Welch, 1967), with segment periodograms computed as the magnitude squared of the Fast Fourier Transform (FFT). Some exemplary time series of groundwater head spectra are depicted in Fig. 1b.

2.2.4 Estimation of Flow Line Length (Fig. 2c)

Using the semi-analytical solution for the spectrum from Liang and Zhang (2013) requires knowledge about the aquifer length L (from water divide to the river intersecting the well location) and the position x of the groundwater observation well along this transect.

The estimation of the flow line length (FLL) is solely based on DEM (digital elevation model) data. Required processing steps are similar to a watershed delineation with geospatial libraries. In a first step, data gaps in the DEM with a resolution of roughly 70x70 m (OpenTopography, 2013) were filled and a flow direction map was calculated providing the drainage direction for each cell. It serves as a basis for calculating the flow accumulation and by that the river network. Within that process, the flow accumulation threshold determines the complexity of the resulting river network. A large threshold (e.g., 1 000) generates a coarser dendritic network and small creeks disappear (purple and blue in Fig. 3). While a smaller value of 100 results in a denser river network with several sub-catchments (orange Fig. 3) and head water catchments (Fig. 3c).

The selection of an appropriate threshold depends not only on the geological and geomorphological context, but also on the intended application of the resulting river network. Setting a low threshold produces a network that includes streams which may be intermittent or even ephemeral (Woessner, 2020). As a result, these streams may not always maintain a connection to the

https://doi.org/10.5194/egusphere-2025-5666
Preprint. Discussion started: 20 November 2025

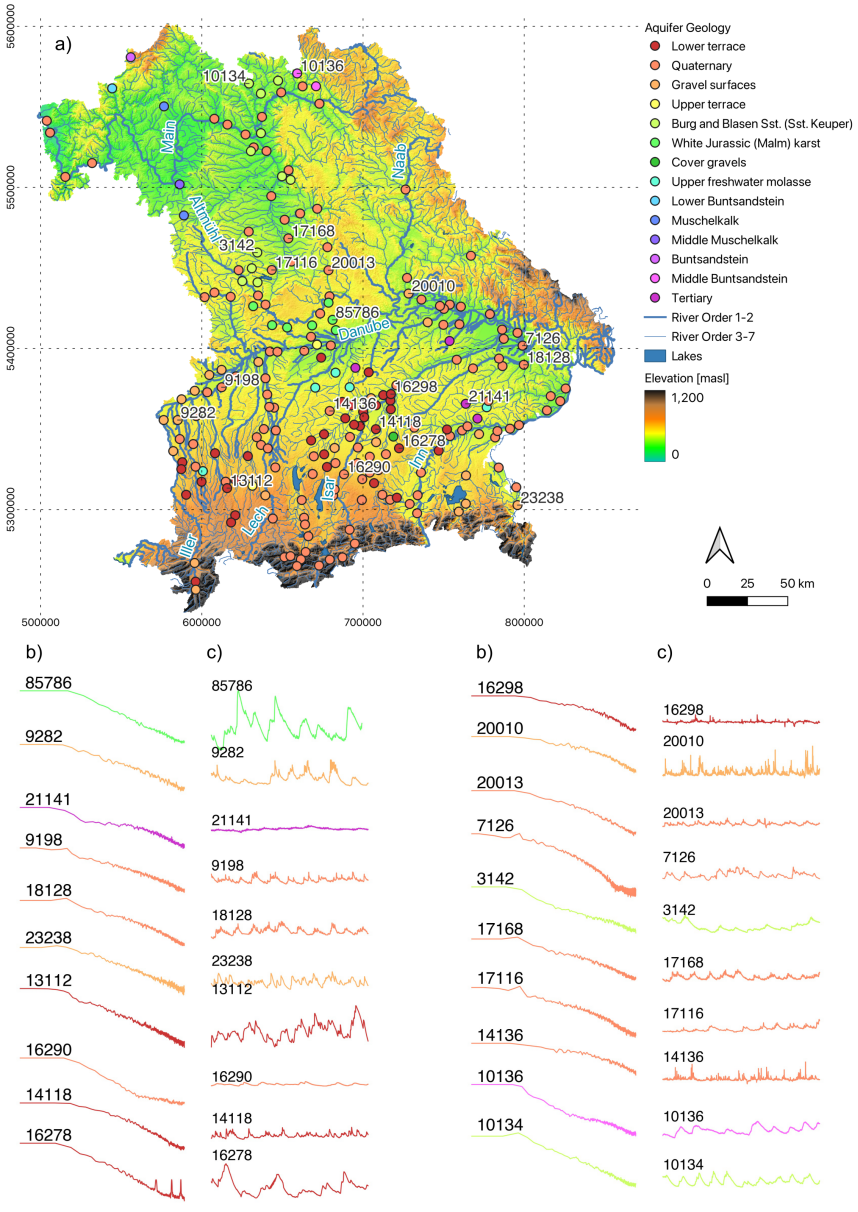

Figure 1. The German state of Bavaria with the locations of the shallow groundwater observation wells from the state monitoring network including their aquifer geology. The digital elevation map was acquired from an SRTM data base (OpenTopography, 2013) while the rivers and lakes were provided by the German Federal Institute for Hydrology (BfG) and downloaded from their geopoartal (German Federal Institute for Hydrology - BfG, 2022). Coordinate reference system EPSG:25832 - ETRS89 / UTM zone 32N.

https://doi.org/10.5194/egusphere-2025-5666
Preprint. Discussion started: 20 November 2025

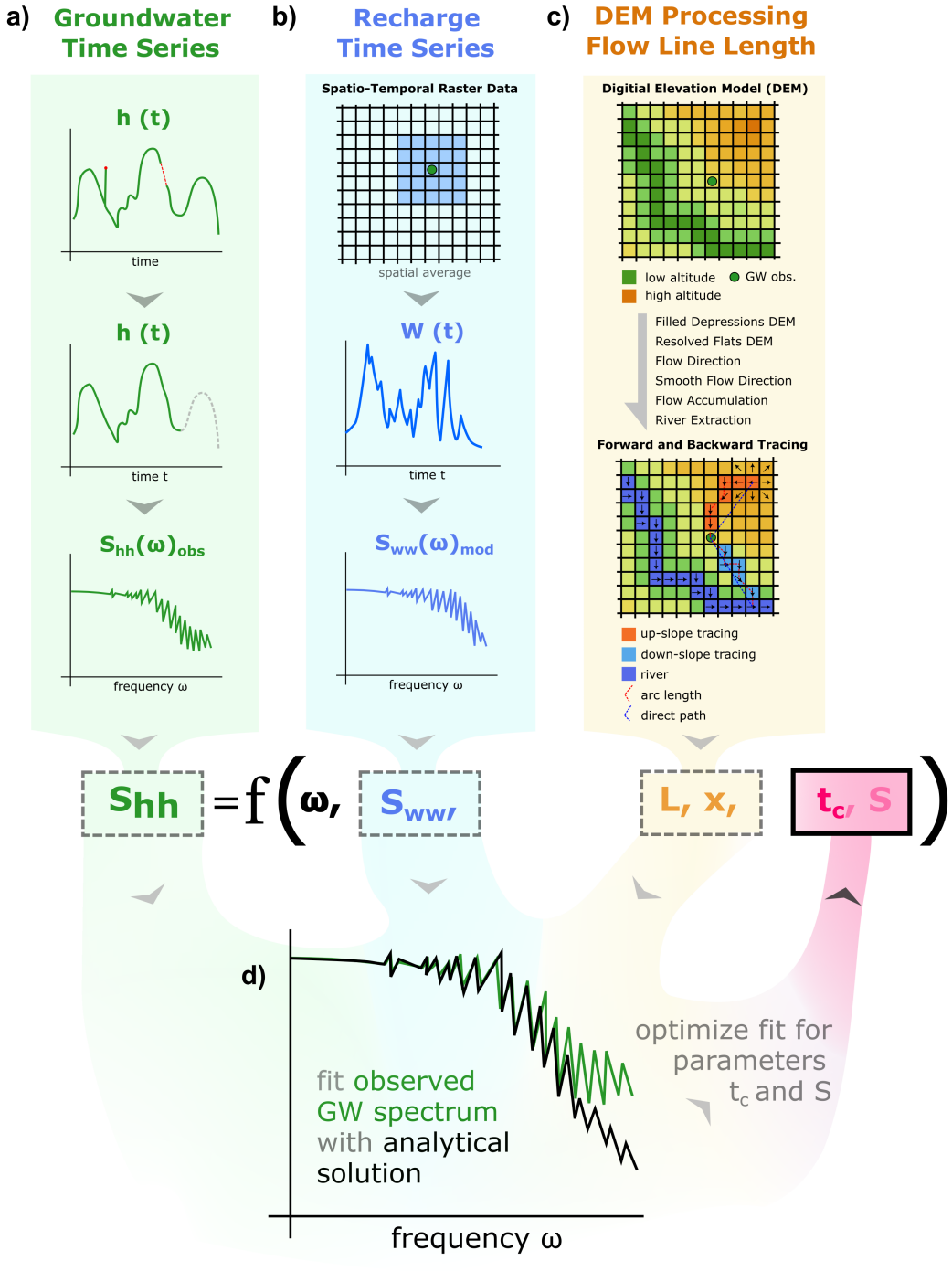

Figure 2. Overview of the spectral analysis (SpA) workflow. The aim is to acquire aquifer parameters based on the spectral representation of groundwater and recharge time series, accompanied by geometric information of the aquifer (flow line lenth) derived from DEM processing.

https://doi.org/10.5194/egusphere-2025-5666
Preprint. Discussion started: 20 November 2025

groundwater table and may not consistently exhibit effluent conditions. This predominantly happens in hilly countrysides with larger depths to the groundwater surface, while in flat areas with shallow groundwater tables, even smaller streams might be directly and continuously connected to the groundwater. We evaluated three thresholds (100, 500 and 1 000) and compared the resulting networks with the official drainage network provided by the German Federal Institute for Hydrology (German Federal Institute for Hydrology - BfG, 2022). A threshold of 1 000 turned out to be the best compromise: The resulting network exhibits the highest agreement with the official drainage network and provides a realistic representation of a river system composed of perennial streams that are regionally well connected to the aquifers. This connectivity is essential for satisfying the boundary conditions of the analytical solution (see Equation 4), to which the spectra will later be fitted.

Next, we approximated the flow lines (FL) by tracing back the path of the water particle starting at the observation well down-slope towards the river (blue, Fig. 2) as well as vice versa, up-slope towards to the water divide (red, Fig. 2). Real groundwater paths can be very complex and are usually unknown without detailed on-site experiments on the catchment scale. Since our study has a regional focus, we decided to use flow direction maps derived from the DEM. Flow direction maps are often very noise, in particular in flat regions. In order to remove noisy patterns, avoid short flow lines and obtain robust estimates, we smoothed the flow direction map (Appendix A1).

The actual path of the water particle along the hill slope (and flow direction) represents the longest path called *arc length* (Fig. 2c, while the shortest and straight distance between summit/river and observation well is called *direct*. For estimating the distance between the observation well and the river, the *direct* distance was applied. A detailed example comparing different FLL can be found in the Appendix A2. The sum of the length of both parts is then equal to the flow line L_{GW} and the length of the upper part determines the location of the groundwater observation well x_{GW} (for water divide $x = 0$ and river $x = L_{GW}$).

The SpA was performed on three different parameter combinations, leading to relatively short, medium and long flow lines. The resulting differences for t_c, x and L are presented in the Appendix as well as results for S and T (Appendix A3 and A4). Since the estimation of t_c once again proved to be robust-showing little sensitivity to the choice of flow lines (Appendix A3), as demonstrated previously by Houben et al. (2022)—we selected a parameterization representative of an intermediate FLL.

2.2.5 Parameter Optimization and Evaluation (Fig. 2d)

Having groundwater level and recharge spectra in addition to estimates for L at hand, the semi-analytical solution was fitted to the observed head spectrum to finally obtain the response time t_c. The fitting of the analytical solution to the observed spectrum was accomplished through an iterative optimization process minimizing least-squares between observed and analytical spectrum to find optimal parameters, t_c and S. Due to the method, the contribution of lower frequencies to the spectra were weighted stronger during optimization than the corresponding ones of higher frequencies. Consequently, the fitted spectra matched better with the observed spectrum for low frequencies (left part in the log-log spectrum plots) while the deviation between both spectra generally appeared at high frequencies (right part of the spectrum plots).

https://doi.org/10.5194/egusphere-2025-5666
Preprint. Discussion started: 20 November 2025

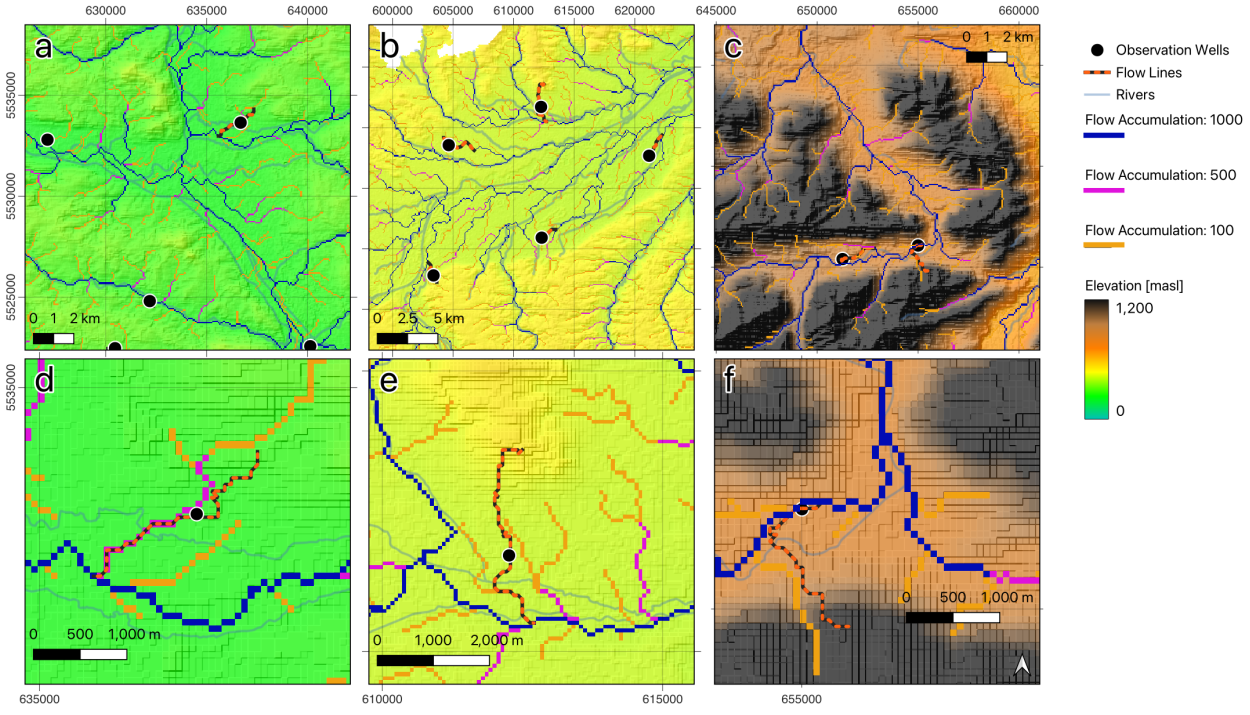

Figure 3. Maps of different geomorphological settings in the study region (a,b,c) showing the resulting river network for different flow accumulation thresholds. The DEM, which was the basis for the watershed analysis, is provided as background map with elevation in meter above sea level (masl). In addition, a river network acquired from the BfG (German Federal Institute for Hydrology - BfG, 2022) is provided to compare it to the extracted river from flow accumulation. (d,e,f) Zoom to three observation wells and their identified flow lines for threshold 1 000 (downward toward the river and upward towards a summit). Depending on the chosen threshold, the flow line would stop earlier or later when it reached a stream.

2.3 Software and Tools

The pre-processing of the time series, as well as other described methods were accomplished by python scripts which will be available via Zenodo upon acceptance of this publication. For the spectral analysis a python library called AquiPy was developed, which is open source and available on GitHub unde this url https://github.com/timohouben/AquiPy and should be referenced via Zenodo (Houben, 2025a).

The AquiPy library allows to handle and pre-process time series (interpolation, detrending), harmonize the recharge and groundwater level time series, calculate the spectra and fit the semi-analytical solution to the observed spectrum of the groundwater levels. Furthermore, the library was used to perform the flow line length estimation based on a digital elevation model (DEM).

https://doi.org/10.5194/egusphere-2025-5666
Preprint. Discussion started: 20 November 2025

3 Results

3.1 Groundwater Level Spectra

209 time series of groundwater levels were analyzed, their spectra were generated and fitted with the analytical solution following the workflow presented in the Fig. 2. Figure 4 depicts a random choice of 48 spectra calculated from observed groundwater level time series (black) and the corresponding fits of the analytical solution $S_{hh\,Fit}$ (blue).

The general shape of most of the spectra is similar, showing a plateau at low frequencies (left part of the spectrum) while gently decreasing for frequencies larger than a specific cut-off frequency. The low frequency regime describes the long time behavior of the groundwater time series. At intermediate frequencies, the onset of the filtering behavior and the response time can be identified. From the mid to the high frequency regime, filtering properties of an aquifer become visible.

Partly there are differences between the spectra for frequencies larger than the cut-off frequency. Visual inspection of these spectra reveals four distinct GoF (Goodness of Fit) categories (Fig. 5). When the observed S_{hh} and theoretical spectra $S_{hh\,Fit}$ exhibit close alignment across the entire frequency range, the result is classified as a *good fit*. If the observed spectrum S_{hh} exhibit steeper slope than anticipated in the theoretical spectrum $S_{hh\,Fit}$ they are labeled as *overestimation*. These spectra show a stronger filter effect leading to generally smoother corresponding groundwater time series. In contrast, for observed spectra S_{hh} with a weaker slope, the fitted spectra $S_{hh\,Fit}$ are *underestimating* the actual conditions, thus representing a groundwater system acting as a weaker filter than anticipated. Lastly, there are spectra that show a second plateau for medium frequencies or intermittent shape which is not reproducible by the theoretical spectrum, therefore labeled as *irregular*.

Approximately 60% of the spectra received the label *good fit*. In these cases, we can conclude that the theoretical model based on the Dupuit approximation captures the dynamic behavior of groundwater very well. Around 15% of the observed groundwater spectra underestimate frequencies larger than 1/30 days (right part of spectrum, see vertical line corresponding to 30 days in Fig. 4), showing a weaker filtering effect that anticipated from the theoretical spectra. Around 19% of observed spectra show an *overestimation* in the mid-range frequency (corresponding to 1 year - 1 month), indicating a stronger filtering effect than in theory. The remaining part, around 5 %, shows *irregular* spectra, where the theoretical spectra deviate across large parts of or even the whole frequency range.

Four examples of time series from groundwater wells, their recharge, the resulting spectra and the results of the SpA can be found in the Appendix A5, A6, A7 and A8.

3.2 Intermediate Frequency Regime: Identification of Aquifer Response Times

Half of the groundwater wells (48 %) show response times between a few days to 100 days, while 28 % have response times between 100 - 200 days. The majority (around 75 %) of the estimated response times from the analyzed aquifers range from approximately 50 days (about 2 months) to 300 days (about 10 months, Fig. 6a which is consistent with the results presented in Kumar et al. (2016).

Two clusters can be identified. A cluster with shorter response times of about 70 to 130 days (2-5 months) and a second cluster with response times ranging approximately from 130 to 340 days (5-10 months). The first cluster predominantly com-

https://doi.org/10.5194/egusphere-2025-5666
Preprint. Discussion started: 20 November 2025

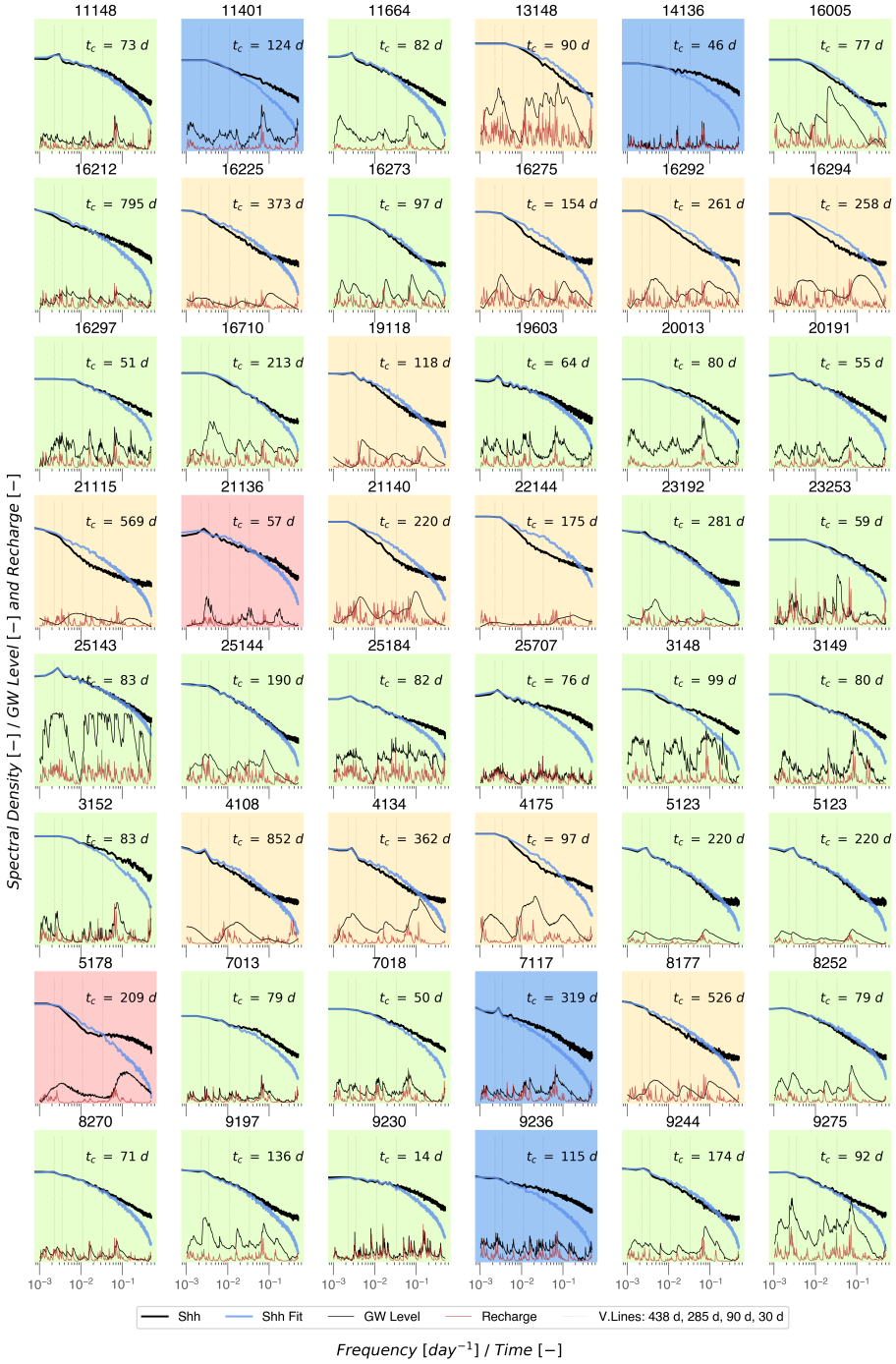

Figure 4. A random choice of 48 groundwater wells from the analysis. Each subplot showing the groundwater level (black line at the bottom), the corresponding spectrum S_{hh} (black spectrum), the extracted and averaged recharge (red line) from which the spectrum S_{ww} was used for the fit of the analytical solution $S_{hh\,Fit}$ (blue spectrum).

https://doi.org/10.5194/egusphere-2025-5666
Preprint. Discussion started: 20 November 2025

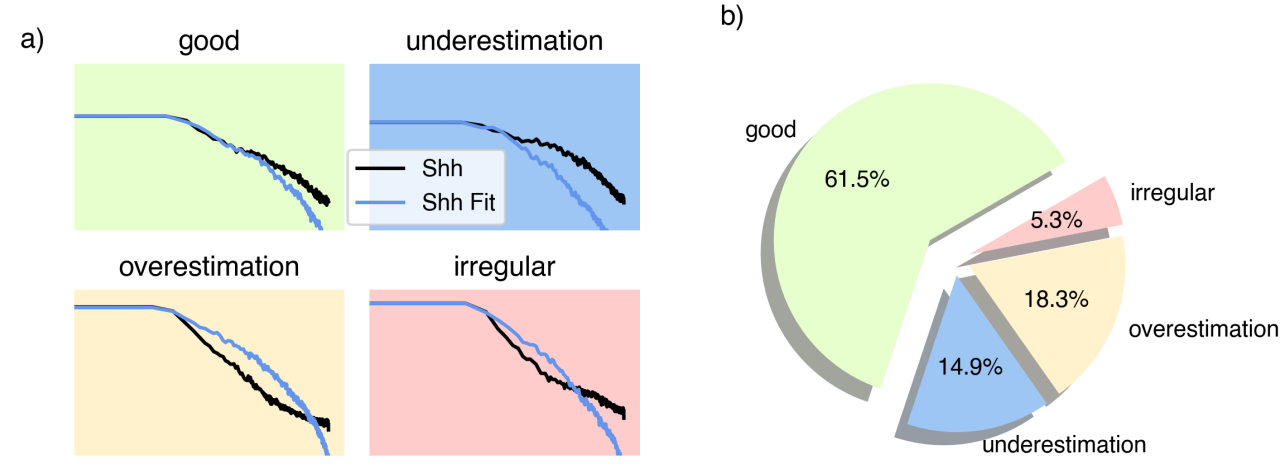

Figure 5. Evaluation of the goodness of the fit. (a) The four categories (*good, underestimation, overestimation, irregular*) and a representative example from the results. (b) Percentage of wells determined for each category.

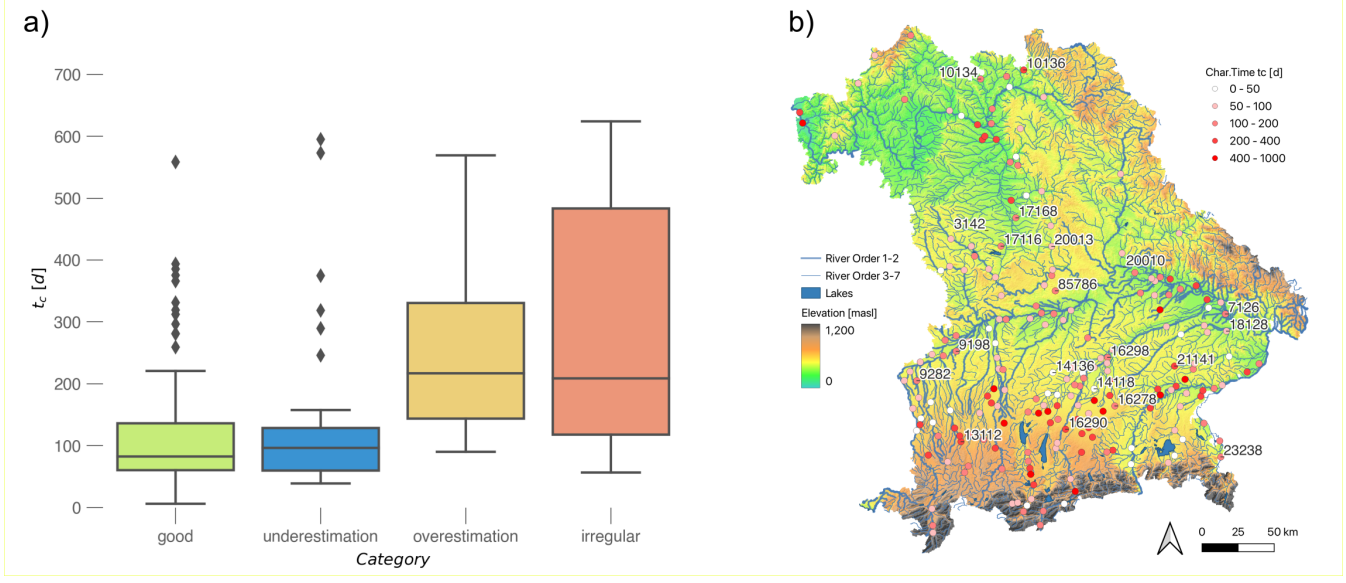

Figure 6. (a) Box plots of resulting aquifer response times for each category. Y-limits were trimmed and three outliers were cut off. (b) Map of Bavaria with SRTM OpenTopography (2013) as basemap and rivers from German Federal Institute for Hydrology - BfG (2022) showing the spatial distribution of obtained t_c.

https://doi.org/10.5194/egusphere-2025-5666
Preprint. Discussion started: 20 November 2025

prises data from shallow groundwater wells (category *good fit, underestimation*, Fig. 7) which show shorter response times, indicating a relatively rapid reaction to recharge events. These wells are predominantly located in unconsolidated Quaternary sedimentary formations such as Lower Terrace and gravel plains, which are characterized by high hydraulic conductivities, facilitating a direct transmission of recharge signals (Fig. 8). In contrast, the second cluster originates from data from deeper groundwater wells (category *overestimation, irregular*, Fig. 7), which exhibit longer response times (Fig. 6), suggesting a more attenuated response to recharge due to the thicker unsaturated zone and deeper flow paths. These wells are commonly located in consolidated formations such as Buntsandstein, Muschelkalk, and the Tertiary, where medium hydraulic conductivities and medium to high storativities result in a stronger damping of high-frequency recharge fluctuations (Fig. 8). A correlation of aquifer geology to the GoF categories could not be identified (Appendix A9).

3.3 High Frequency Regime: Filtering Behavior

Groundwater level fluctuations characterized by less high-frequency content (category *overestimation*, indicating a stronger filter) tend to occur at greater depths, whereas fluctuations containing more high-frequency components (category *underestimation*, weaker filter) are generally associated with shallower water tables. This behavior is illustrated by maps in Fig. 9. The left panel presents wells for which the theoretical spectra showed a good fit to the observed spectra. These wells are distributed throughout Bavaria and exhibit the full range of depths to the water table.

The middle panel, representing the *underestimation* cases, consists predominantly of wells with shallow water tables. Underestimation occurs when the model does not fully capture the high-frequency variability, for example due to a dynamic groundwater recharge with more short-term fluctuations than assumed in the semi-analytical solution. Despite this limitation, the method still provides a good estimate for mid-range frequencies and with that groundwater response times on monthly to seasonal scales. Consequently, the inferred characteristic response time t_c remains a robust estimate.

The right panel highlights *overestimation* cases, which occur mainly in the southern and more elevated parts of the study area, where deeper groundwater tables are prevalent. Overestimation is observed in around 18 % of cases, where the semi-analytical solution predicts greater short-term variability than observed, indicating a stronger filtering effect than in reality. This could result from missing mid-term variability in the input signal (recharge) or unaccounted storage effects that further dampen mid-term fluctuations.

While the Transmissivity T and Storativity S are outcomes of the fitting workflow, they have not been discussed in detail in this study. The reason for this decision is that previous research (Houben et al., 2022) has demonstrated that especially T is highly sensitive to the the length of flow line ($FLL = L$, see Equation 6), leading to considerable uncertainties in their estimation (Appendix A4). Therefore, we suggest further studies to improve the accuracy of the estimation of the FLL and the recharge time series. Additionally, considering lateral groundwater flow or aquifer leakage might enhance the predictive power of the semi-analytical solution, though this data are difficult to acquire and hard to integrate into analytical solutions. Exploratory modeling approaches incorporating leakage or lateral inflows could quantify these influences and their sensitivity within the spectral approach.

https://doi.org/10.5194/egusphere-2025-5666
Preprint. Discussion started: 20 November 2025

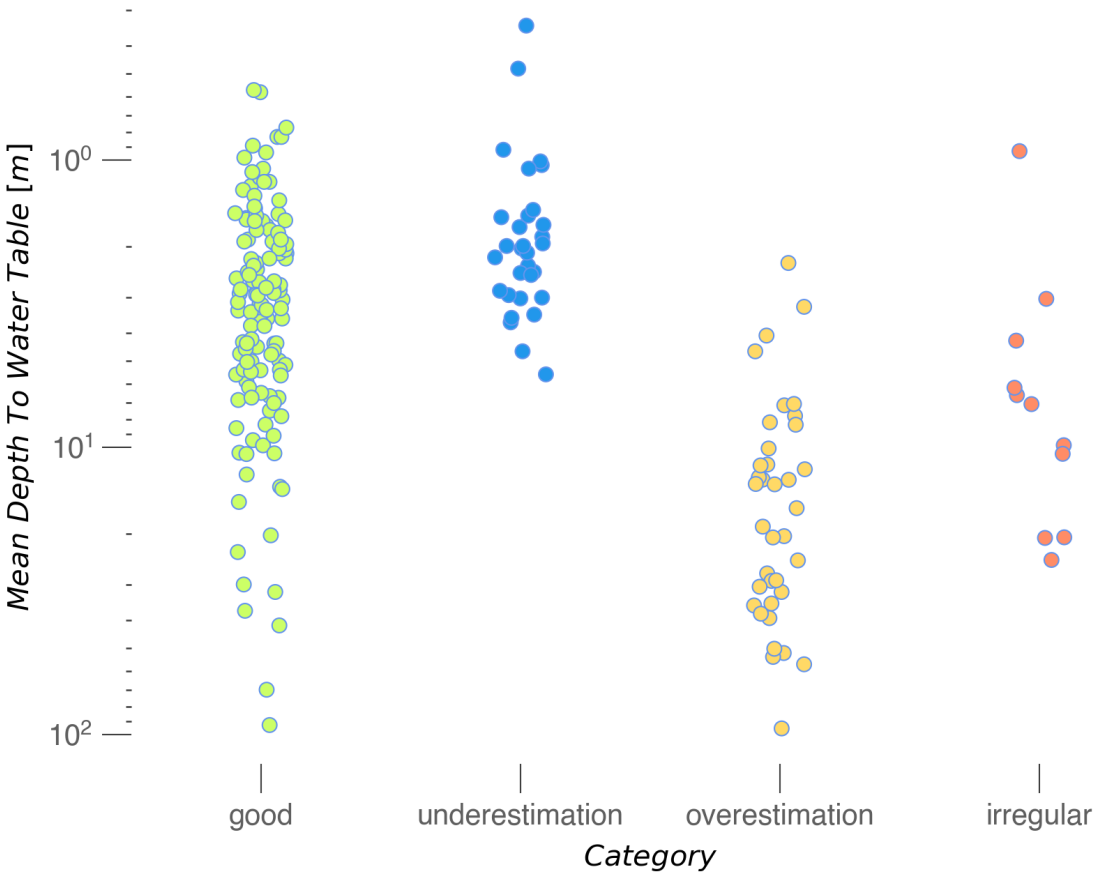

Figure 7. The four categories of the GoF in relation to the mean depth to the groundwater table. Good fitting spectra appear for across all depths. Shallow wells tend to be underestimated while deeper wells tend to be overestimated.

https://doi.org/10.5194/egusphere-2025-5666
Preprint. Discussion started: 20 November 2025

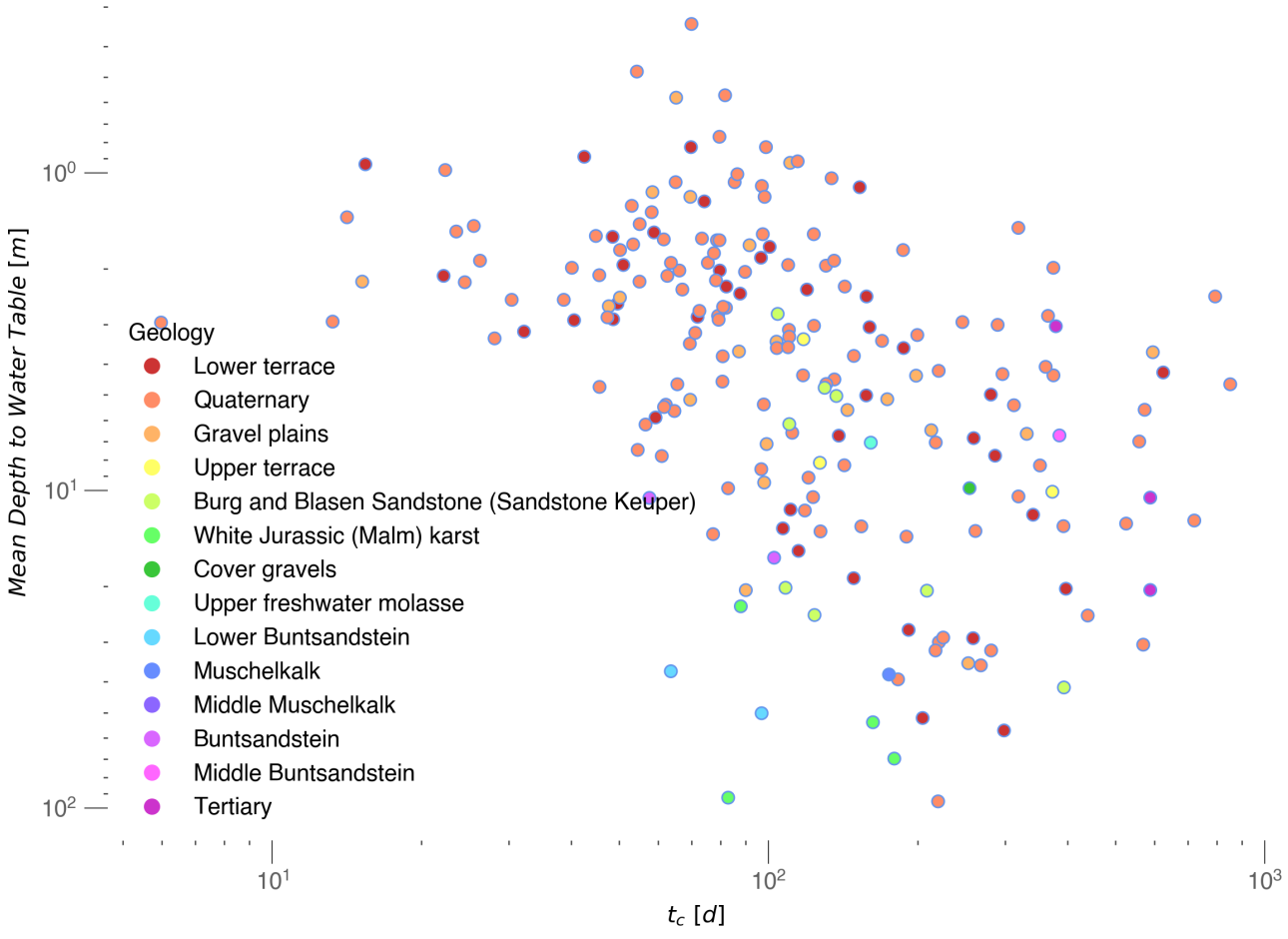

Figure 8. Scatter plot of depth to the water table (m) versus aquifer response time t_c (days), categorized by aquifer geology. Each point represents a groundwater well, with colors indicating different aquifer types.

https://doi.org/10.5194/egusphere-2025-5666
Preprint. Discussion started: 20 November 2025

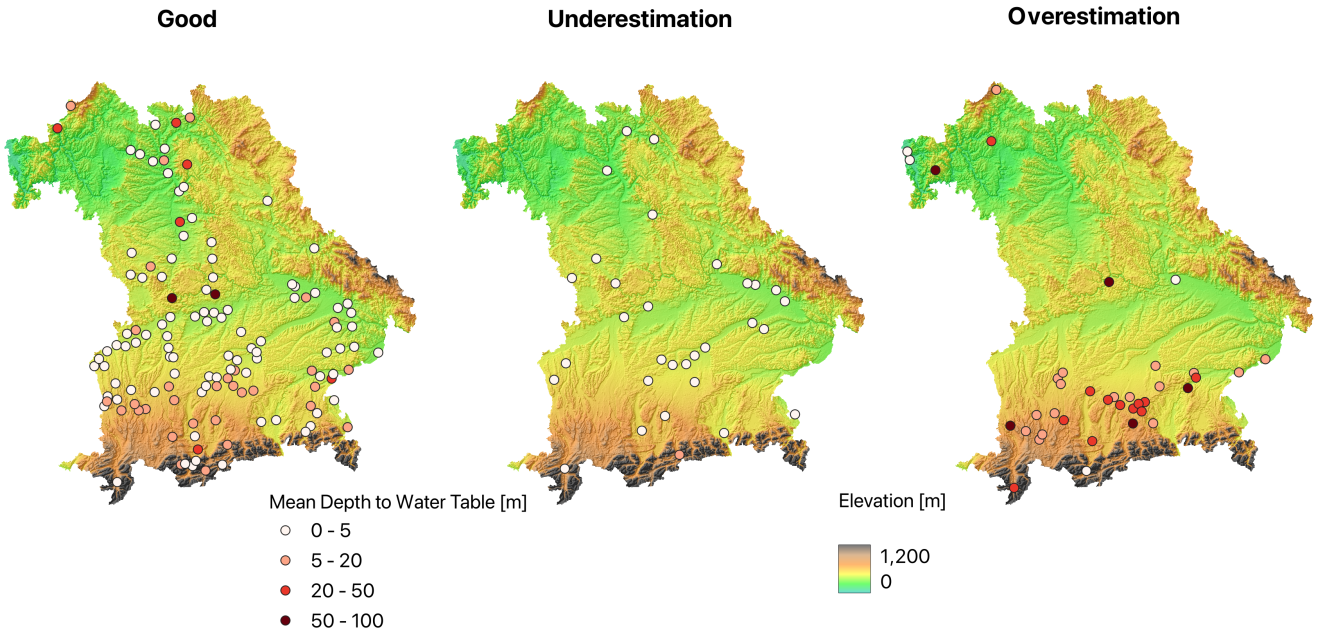

Figure 9. Spatial distribution of wells separated by GoF (Goodness of Fit) categories. The well locations are plotted together with the elevation map and markers for the GW wells, which are color-coded by depth to the water table.

4 Discussion

This study introduces a novel spectral analysis method as part of a workflow to estimate characteristic response times of groundwater systems. These response times reflect how rapidly groundwater levels respond to changes in recharge or extraction and serve as a critical indicator of aquifer resilience under climatic and anthropogenic stresses. We applied this approach to approximately 200 groundwater level time series across southern Germany, integrating modeled recharge data and hydrogeomorphic parameters derived from digital elevation models. Our findings demonstrate that the semi-analytical spectral solution generally provides a strong fit to observed groundwater spectra and allows robust estimation of response times, which predominantly range from 50 to 300 days across shallow Bavarian aquifers ($>$ 100 m depth).

Within groundwater level spectra, three frequency regimes are distinguished. The low-frequency regime corresponds to long-term seasonal behavior, while intermediate frequencies reveal the onset of filtering related to the groundwater response time. The high-frequency regime exposes the aquifer's filtering properties. While the model fits most spectra well, deviations primarily occur in the high-frequency regime (corresponding to less than 30 days period), which suggests the semi-analytical solution may not fully capture rapid recharge fluctuations or effects of processes such as anthropogenic withdrawals and lateral groundwater flow.

At locations with stronger filtering than estimated (*overestimation*), actual groundwater recharge dynamics may be less variable than modeled by the mesoscale hydrological model mHM. Conversely, weaker filtering behavior (*underestimation*)

https://doi.org/10.5194/egusphere-2025-5666
Preprint. Discussion started: 20 November 2025

likely indicates more dynamic recharge fluctuations than anticipated. These observations highlight potential limitations of the recharge inputs and imply that the method may also serve as a tool for evaluating distributed hydrological models.

The estimated characteristic response times align well with previous studies (Houben et al., 2022; Boumaiza et al., 2021; Kumar et al., 2016). Generally, deeper groundwater tables correspond to longer response times, implying greater resilience to droughts through higher buffering capacity. Shallow systems respond more quickly to recharge changes and are more vulnerable to extended dry periods, underscoring the relevance of aquifer depth in resilience assessments.

Comparing groundwater response times with drought durations is essential. Short response times may lead to rapid water table declines during dry seasons, while long response times correspond to prolonged aquifer recovery, maintaining low-water conditions. Given climate change-induced increases in drought frequency and severity, flexible and regionally targeted groundwater management strategies are critical.

While response time provides valuable insight into aquifer resilience, additional indicators are necessary for a comprehensive assessment. We propose incorporating metrics such as the duration of water storage in the subsurface, beside information on water abstraction rates. Future work will focus on identifying storativity S alongside t_c in order to evaluate the aquifer resilience comprehensively and quantifying associated uncertainties.

Overall, this spectral approach proves to be a powerful tool for characterizing groundwater system dynamics and offers important implications for assessing aquifer resilience under changing climatic conditions.

5 Conclusions

This study successfully demonstrates that spectral analysis of groundwater levels with semi-analytical solutions, can robustly estimate characteristic response times across a large number of aquifers. Groundwater response times predominantly range between 50 and 300 days in the studied Bavarian systems. The semi-analytical solution for the spectral domain applies well to the majority of investigated groundwater time series. Furthermore, the correlation between groundwater depth and spectral filtering underlines the importance of aquifer characteristics in quantifying resilience to drought and recharge variability.

Incorporation of additional anthropogenic and hydrological factors, such as withdrawal rates, as well as improvements of FLL estimations, is needed to further refine the estimation of aquifer parameters, including transmissivities and storativities.

Future research will extend these methods to include storage estimation, improving our understanding of aquifer vulnerability and informing water resource management in a changing climate.

Code and data availability. The groundwater level data used in this study were provided by the Bavarian State Office for the Environment (LfU) representing the upper groundwater storey (groundwater table depth smaller than 100 m). The selected time series were downloaded via the online service https://www.gkd.bayern.de/de/grundwasser/oberesstockwerk (Bayerisches Landesamt für Umwelt, 2022). The recharge data was produced with the mHM hydrological model (Marx et al., 2021). The digital elevation map was acquired from an SRTM data base (OpenTopography, 2013) while the rivers and lakes were provided by the German Federal Institute for Hydrology (BfG) and downloaded from their geoportal (German Federal Institute for Hydrology - BfG, 2022). The data which were finally used within the scope of this study

https://doi.org/10.5194/egusphere-2025-5666
Preprint. Discussion started: 20 November 2025

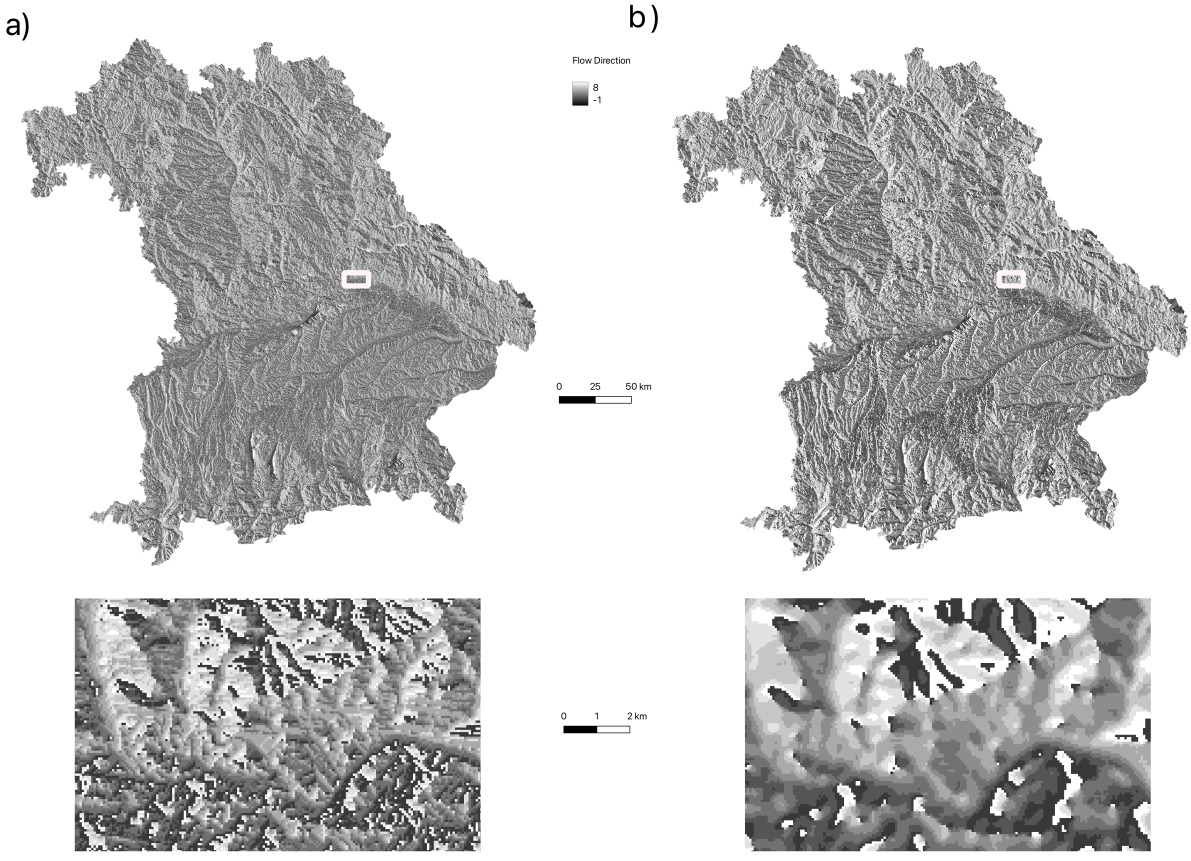

Figure A1. (a) Standard flow direction map derived from a DEM, (b) smoothed flow direction map. The flow direction was smoothed with a python function by averaging neighboring direction vectors over a specified "level" of neighborhood. Here, level 2 was used, meaning that two levels of surrounding cells where included, mapping back the average value to the center cell. The corresponding code can be found in the AquiPy package on GitHub https://github.com/timohouben/AquiPy.

are available on Zenodo (Houben, 2025b). This upload also contains workflow scripts required for the reproduction of the results of this study. The scripts are based on the AquiPy python library which was developed for the analysis. The package is available on GitHub under this url https://github.com/timohouben/AquiPy and should be referenced via the corresponding Zenodo publication (Houben, 2025a).

https://doi.org/10.5194/egusphere-2025-5666
Preprint. Discussion started: 20 November 2025

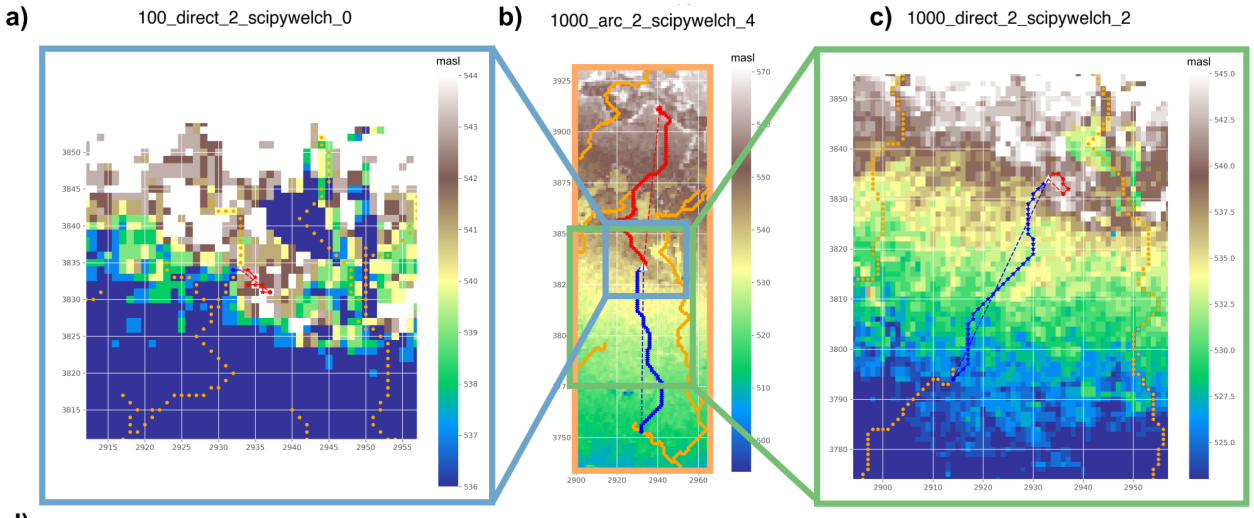

d)

Combination	Characteristic Time tc [days]	Distance to Water Divide x [m]	Aquifer Length L [m]	Storativity S [-]	Transmissivity T [m²/s]
100_direct_2_scipywelch_0	80	350	420	1.64e-02	4.21e-04
1000_arc_2_scipywelch_4	78	7324	13791	3.77e-02	1.06e+00
1000_direct_2_scipywelch_2	77	297	3403	5.09e-02	8.81e-02

Figure A2. Resulting flow lines for three different parameter sets. (a) Flow lines generated with the smallest flow accumulation threshold (100), resulting in the shortest flow paths. Streams extend far into the hills, reducing the distance from the well to the nearest river (blue lines). With no smoothing applied to the flow direction, the upstream path terminates early (red lines). (b) The longest flow lines, produced using a higher flow accumulation threshold (1000). Here, rivers appear less dendritic, and the distance from the well to the river increases. Strong smoothing of the flow direction (level 4) causes the upstream segment to reach higher elevations. The arc length (indicated by stars) is used to measure the path, in contrast to the direct connection (dashed lines). (c) A parameter set that yields flow lines of intermediate length, which is selected for further analysis in this study. (d) A table summarizing the key values for each parameter set. The distance to the water divide x represents the distance from the well to the water divide. The aquifer length L is defined as the sum of the upstream and downstream segments.

Appendix A: Additional Figures

Author contributions. Conceptualization: TH, SA, Methodology: TH, CS, TK, MdD, TF, Software: TH, Validation: TH, Formal analysis: TH, Resources: CS, SA, Data curation: TH, Writing: original draft: TH, SA, CS, TK, TF, Visualization: TH, Supervision: SA, CS, TK, Project administration: SA, Funding acquisition: SA

Competing interests. The authors declare no competing interests.

https://doi.org/10.5194/egusphere-2025-5666
Preprint. Discussion started: 20 November 2025

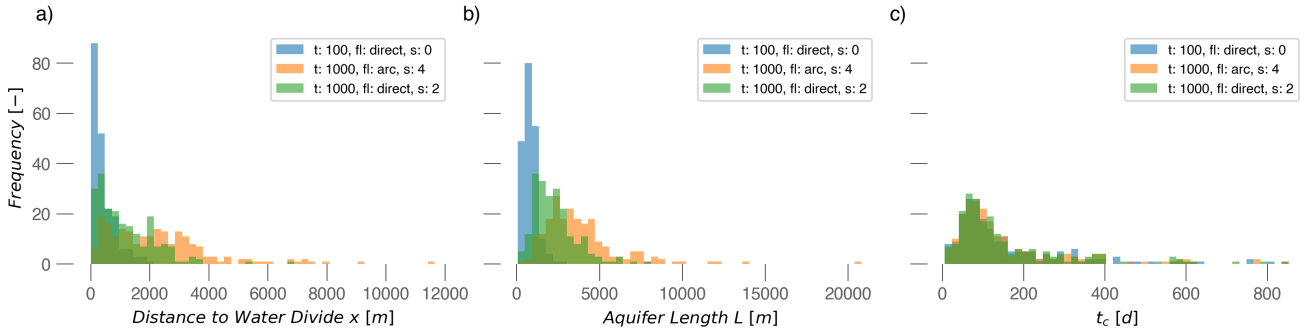

Figure A3. Flow line estimation results and spectral analysis results for three different parameter configurations. (a) Distance to water divide x and (b) aquifer length L as a result of the Flow Line Length estimation with different flow accumulation thresholds t, selection of flow lines fl and smoothed flow direction map s. Short flow lines are created when the flow accumulation threshold is small, because a dendritic river network is created. Direct flow lines connect the starting and end point of the flow lines with a straight line, while the arc length follows the whole flow path along the hillslope (i.e. the DEM). The higher the number for the smoothing of the flow lines, the longer the flow paths. (c) Resulting characteristic time t_c for the three parameter sets.

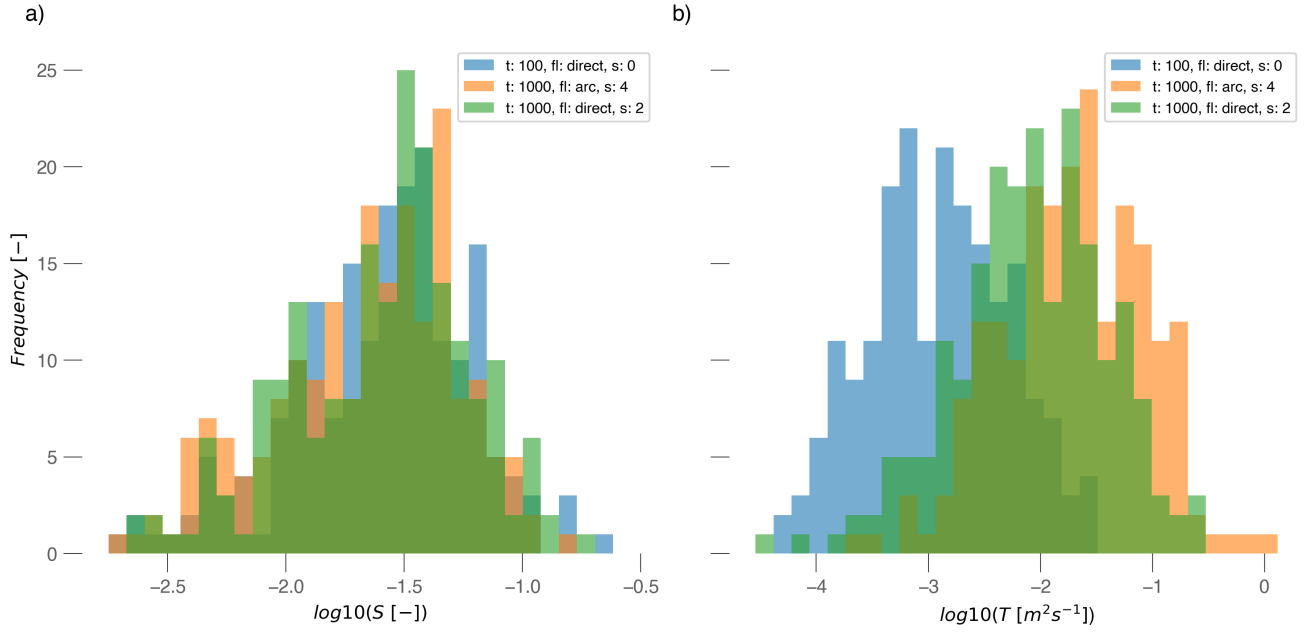

Figure A4. spectral analysis results for the three parameter sets for the flow line estimation. (a) storativity S and (b) transmissivity T. While resulting storativities differ only slightly, the transmissivities show stronger deviations due to different flow line lengths (=aquifer length) L.

https://doi.org/10.5194/egusphere-2025-5666
Preprint. Discussion started: 20 November 2025

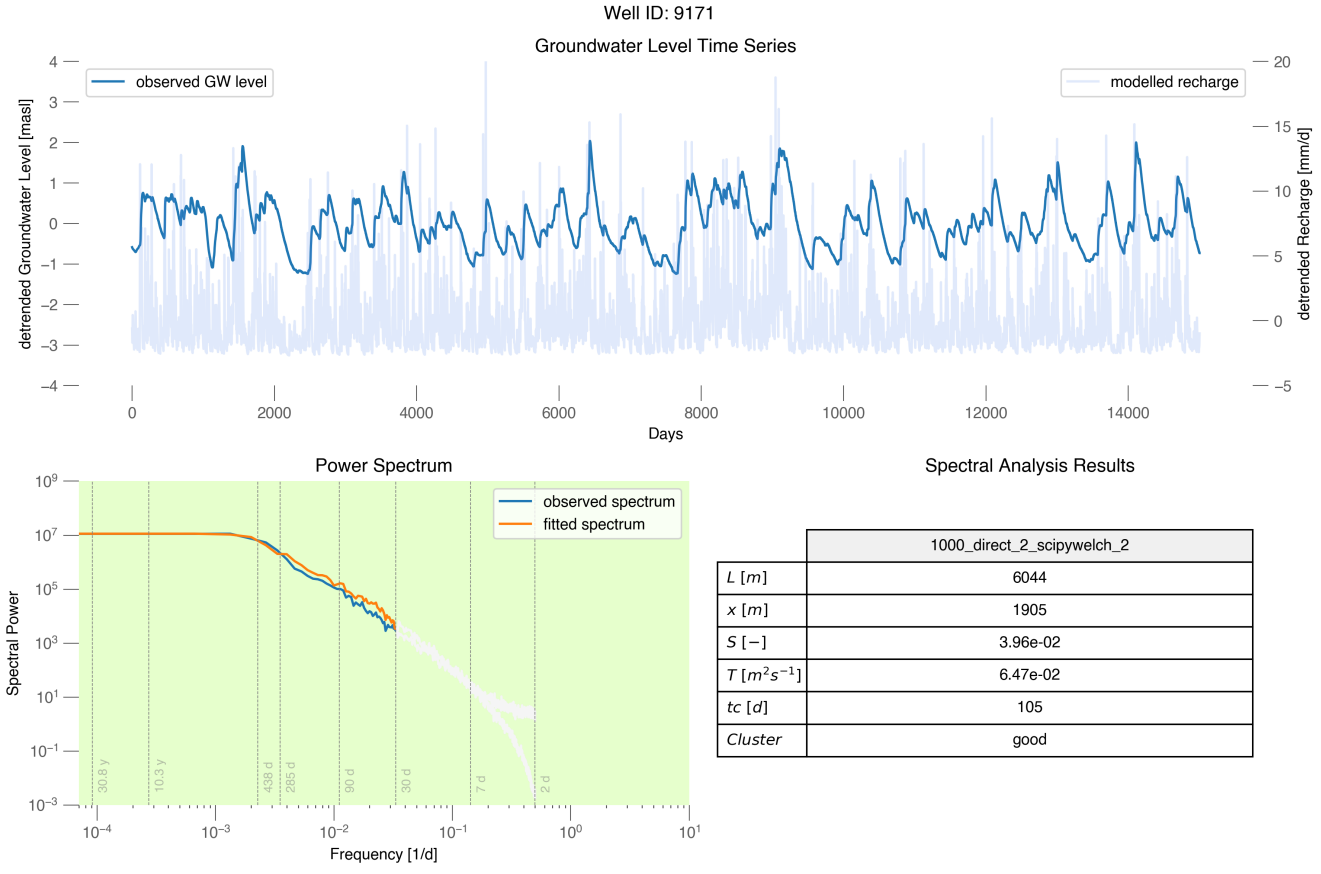

	1000_direct_2_scipywelch_2
$L\ [m]$	6044
$x\ [m]$	1905
$S\ [-]$	3.96e-02
$T\ [m^2 s^{-1}]$	6.47e-02
$tc\ [d]$	105
Cluster	good

Figure A5. An example of a summary of analysis for a groundwater well of the category *good fit*. The figure shows the observed groundwater level time series and the modeled mHM recharge Marx et al. (2021), the resulting power spectra for the observed groundwater level and the fitted spectrum with the semi-analytical solution. Only the colored part of the spectrum up to a frequency corresponding to 30 d was taken for the goodness of fit evaluation. The table summarizes the results of the workflow for the selected parameter set.

https://doi.org/10.5194/egusphere-2025-5666
Preprint. Discussion started: 20 November 2025

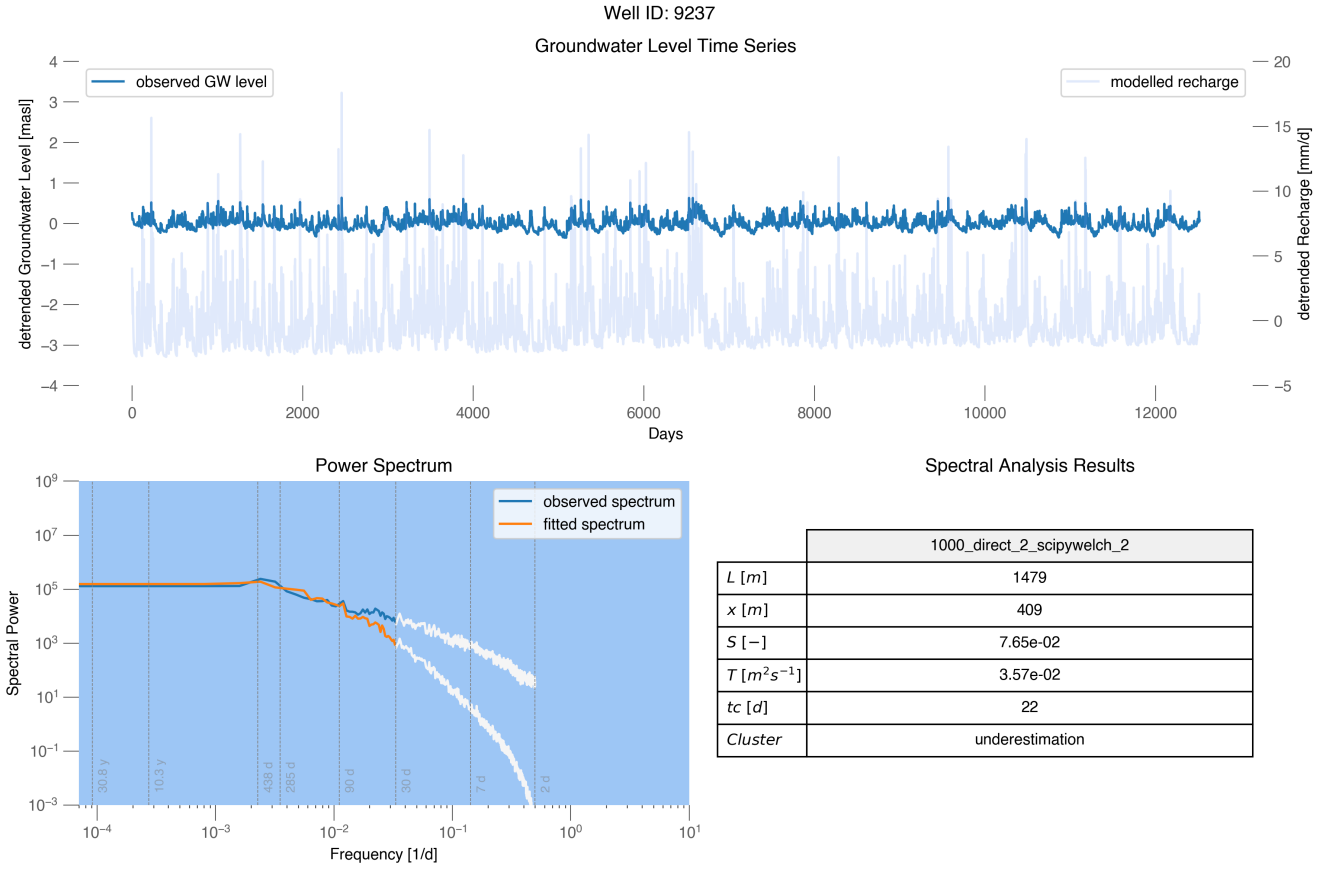

Spectral Analysis Results

	1000_direct_2_scipywelch_2
$L\ [m]$	1479
$x\ [m]$	409
$S\ [-]$	7.65e-02
$T\ [m^2 s^{-1}]$	3.57e-02
$tc\ [d]$	22
Cluster	underestimation

Figure A6. An example of a summary of analysis for a groundwater well of the category *underestimation*. The figure shows the observed groundwater level time series and the modeled mHM recharge Marx et al. (2021), the resulting power spectra for the observed groundwater level and the fitted spectrum with the semi-analytical solution. Only the colored part of the spectrum up to a frequency corresponding to 30 d was taken for the goodness of fit evaluation. The table summarizes the results of the workflow for the selected parameter set.

https://doi.org/10.5194/egusphere-2025-5666
Preprint. Discussion started: 20 November 2025

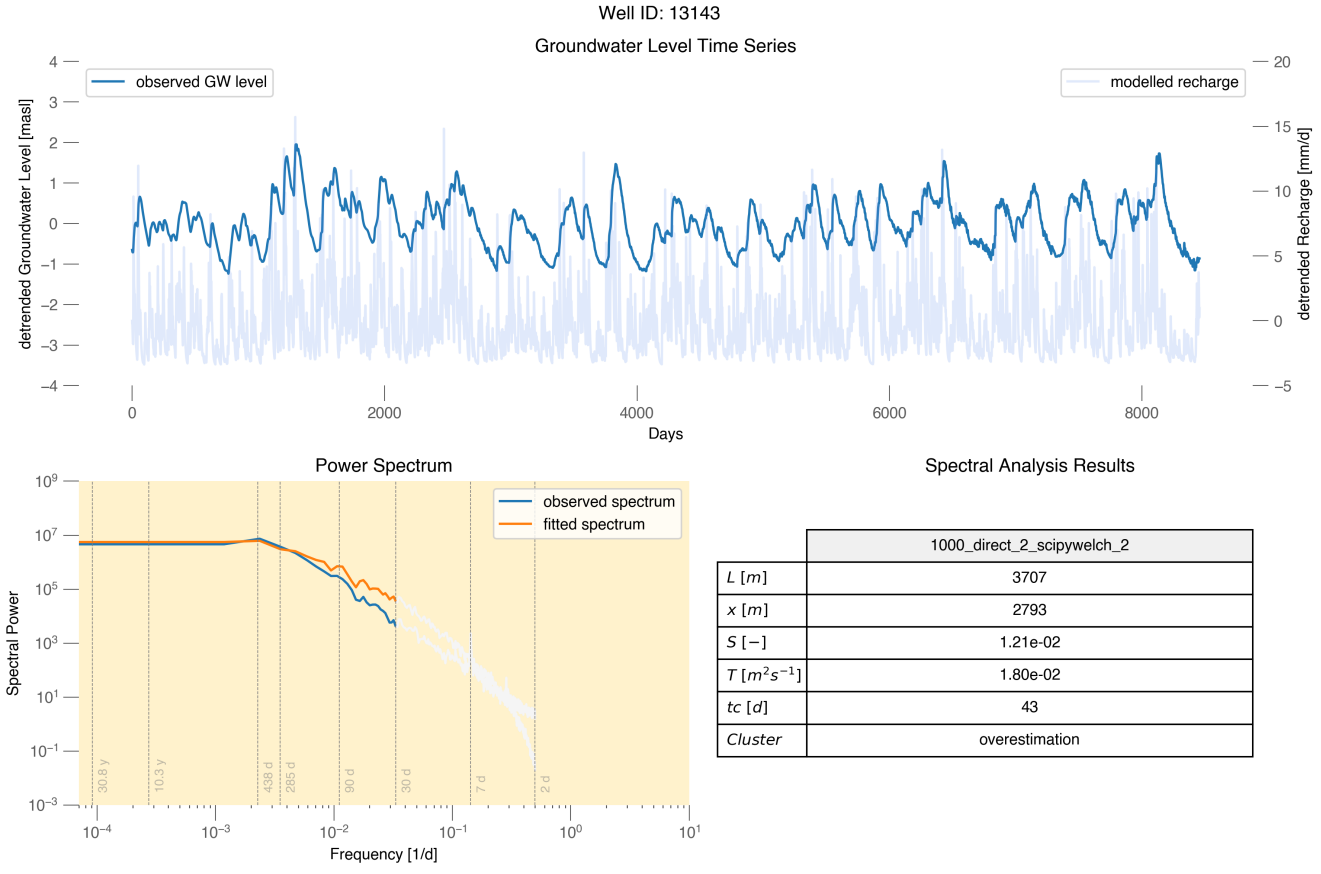

	1000_direct_2_scipywelch_2
$L\ [m]$	3707
$x\ [m]$	2793
$S\ [-]$	1.21e-02
$T\ [m^2 s^{-1}]$	1.80e-02
$tc\ [d]$	43
Cluster	overestimation

Figure A7. An example of a summary of analysis for a groundwater well of the category *overestimation*. The figure shows the observed groundwater level time series and the modeled recharge mHM Marx et al. (2021), the resulting power spectra for the observed groundwater level and the fitted spectrum with the semi-analytical solution. Only the colored part of the spectrum up to a frequency corresponding to 30 d was taken for the goodness of fit evaluation. The table summarizes the results of the workflow for the selected parameter set.

https://doi.org/10.5194/egusphere-2025-5666
Preprint. Discussion started: 20 November 2025

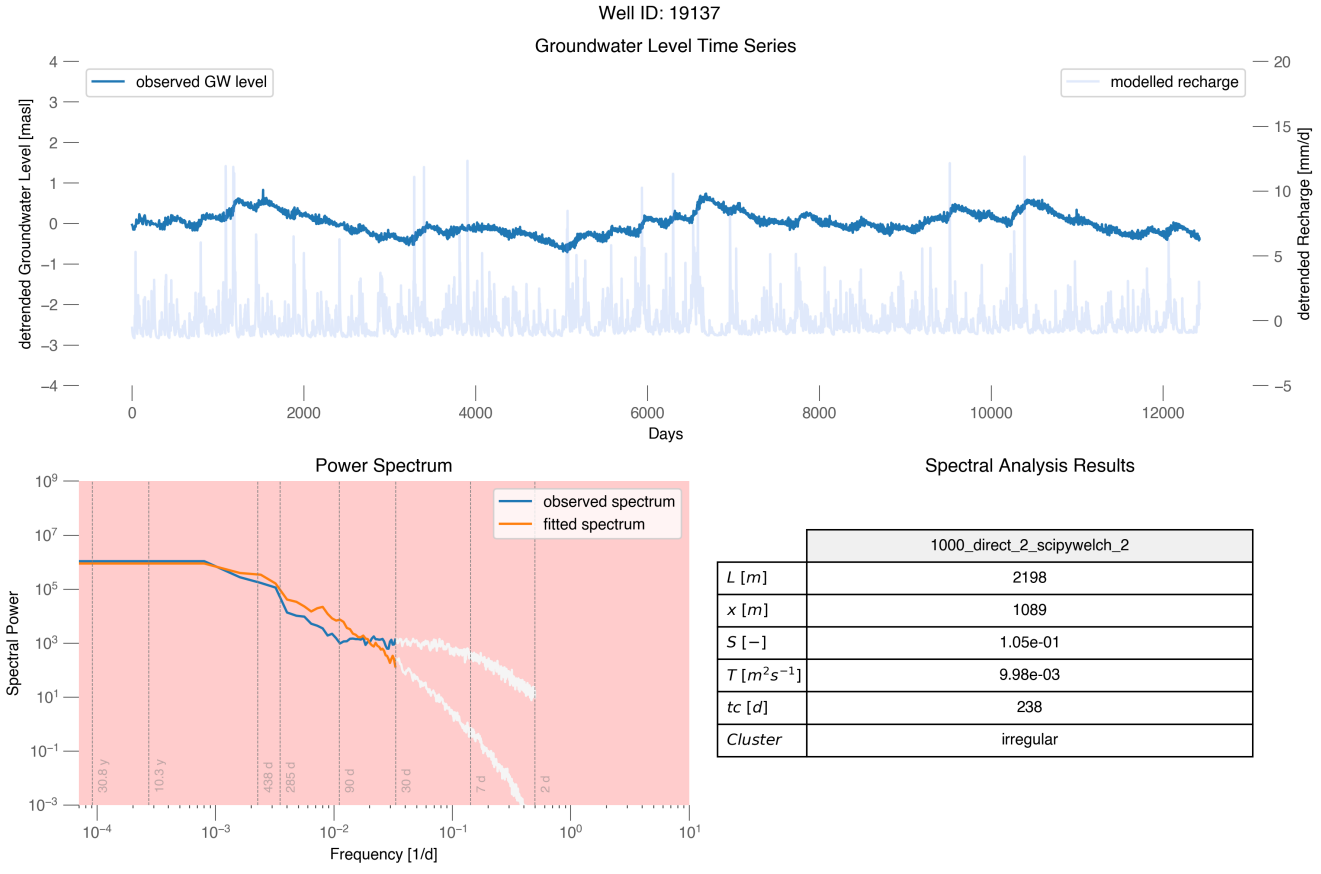

Spectral Analysis Results

	1000_direct_2_scipywelch_2
$L\ [m]$	2198
$x\ [m]$	1089
$S\ [-]$	1.05e-01
$T\ [m^2 s^{-1}]$	9.98e-03
$tc\ [d]$	238
Cluster	irregular

Figure A8. An example of a summary of analysis for a groundwater well of the category *irregular*. The figure shows the observed groundwater level time series and the modeled mHM recharge Marx et al. (2021), the resulting power spectra for the observed groundwater level and the fitted spectrum with the semi-analytical solution. Only the colored part of the spectrum up to a frequency corresponding to 30 d was taken for the goodness of fit evaluation. The table summarizes the results of the workflow for the selected parameter set.

https://doi.org/10.5194/egusphere-2025-5666
Preprint. Discussion started: 20 November 2025

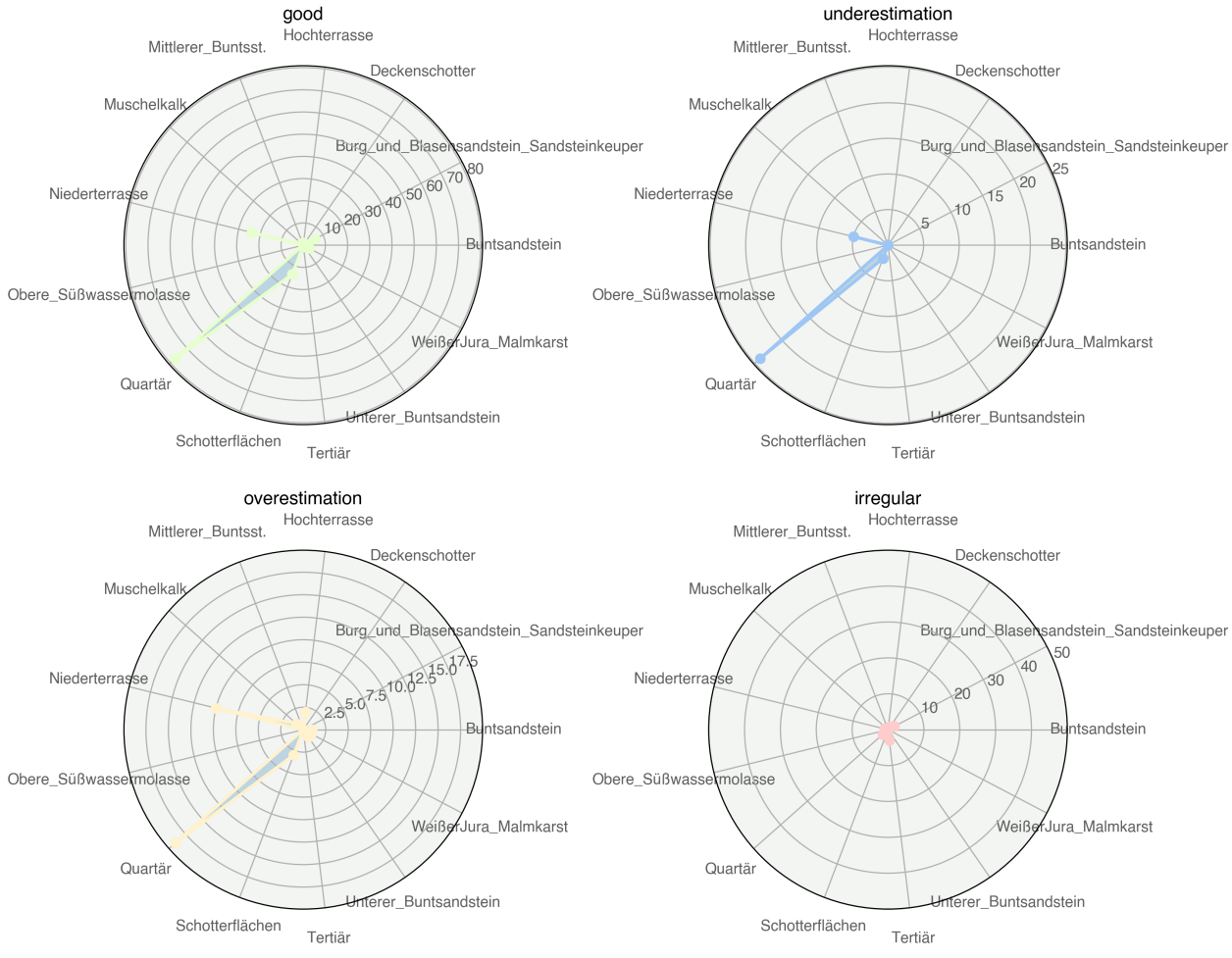

Figure A9. Spider plots showing the aquifer geology for the four GoF (goodness of fit) categories.

https://doi.org/10.5194/egusphere-2025-5666
Preprint. Discussion started: 20 November 2025

Acknowledgements. This work was funded by the Helmholtz Centre for Environmental Research (UFZ) in Leipzig. We would like to thank the GH2O group of the LandTrans initiative at UFZ for feedback, support and extensive discussion. The scientific results have been computed at the High-Performance Computing (HPC) Cluster EVE, a joint effort of both the Helmholtz Centre for Environmental Research - UFZ (https://www.ufz.de/) and the German Centre for Integrative Biodiversity Research (iDiv) Halle-Jena-Leipzig (http://www.idiv-biodiversity.de/). Furthermore, we would like to thank Andreas Marx and Friedrich Boeing for providing the groundwater recharge data. The authors would like to thank three anonymous reviewers for constructive feedback which improved the quality of this paper. Different large language models were used to improve the language of the paper and supported the code production for the presented analysis.

https://doi.org/10.5194/egusphere-2025-5666
Preprint. Discussion started: 20 November 2025

References

Bayerisches Landesamt für Umwelt: Oberes Grundwasser-Stockwerk Bayern, https://www.gkd.bayern.de/de/grundwasser/oberesstockwerk, 2022.

Bear, J.: Dynamics of fluids in porous media, American Elsevier Pub. Co, New York, ISBN 044400114X, https://doi.org/10.1097/00010694-197508000-00022, 1972.

Boumaiza, L., Chesnaux, R., Walter, J., and Meghnefi, F.: Assessing response times of an alluvial aquifer experiencing seasonally variable meteorological inputs, Groundwater for Sustainable Development, 14, 100 647, https://doi.org/10.1016/j.gsd.2021.100647, 2021.

Brutsaert, W.: Long-term groundwater storage trends estimated from streamflow records: Climatic perspective, Water Resources Research, 44, https://doi.org/10.1029/2007wr006518, 2008.

Carr, E. J. and Simpson, M. J.: Accurate and efficient calculation of response times for groundwater flow, Journal of Hydrology, 558, 470–481, https://doi.org/https://doi.org/10.1016/j.jhydrol.2017.12.023, 2018.

Ciscar, J.-C., Rising, J., Kopp, R. E., and Feyen, L.: Assessing future climate change impacts in the EU and the USA: insights and lessons from two continental-scale projects*, Environmental Research Letters, 14, 084 010, https://doi.org/10.1088/1748-9326/ab281e, 2019.

Cuthbert, M. O., Gleeson, T., Moosdorf, N., Befus, K. M., Schneider, A., Hartmann, J., and Lehner, B.: Global patterns and dynamics of climate–groundwater interactions, Nature Climate Change, 9, 137–141, https://doi.org/10.1038/s41558-018-0386-4, 2019.

de Rooij, G. H.: Transient flow between aquifers and surface water: analytically derived field-scale hydraulic heads and fluxes, Hydrology and Earth System Sciences, 16, 649–669, https://doi.org/10.5194/hess-16-649-2012, 2012.

de Rooij, G. H.: Aquifer-scale flow equations as generalized linear reservoir models for strip and circular aquifers: Links between the Darcian and the aquifer scale, Water Resources Research, 49, 8605–8615, https://doi.org/10.1002/2013wr014873, 2013.

Erskine, A. and Papaioannou, A.: The use of aquifer response rate in the assessment of groundwater resources, Journal of Hydrology, 202, 373–391, https://doi.org/10.1016/s0022-1694(97)00058-9, 1997.

European Commission, J. R. C.: Droughts in Europe and Worldwide 2019-2020, Publications Office, LU, ISBN 978-92-76-38040-5, https://doi.org/10.2760/415204, 2021.

Freeze, R.: Groundwater, Prentice-Hall, Englewood Cliffs, N.J, ISBN 0133653129, 1979.

Fritsch, F. N. and Carlson, R. E.: Monotone Piecewise Cubic Interpolation, SIAM Journal on Numerical Analysis, 17, 238–246, https://doi.org/10.1137/0717021, 1980.

Gelhar, L. W. and Wilson, J. L.: Ground-Water Quality Modeling, Ground Water, 12, 399–408, https://doi.org/10.1111/j.1745-6584.1974.tb03050.x, 1974.

German Federal Institute for Hydrology - BfG: Waterbody DE, https://geoportal.bafg.de/CSWView/od.xhtml, 2022.

Hameed, M., Nayak, M. A., and Ahanger, M. A.: Event-Based Recession Analysis for Estimation of Basin-Wide Characteristic Drainage Timescale and Groundwater Storage Trends, Water Resources Research, 59, https://doi.org/10.1029/2023wr035829, 2023.

Hellwig, J. and Stahl, K.: An assessment of trends and potential future changes in groundwater-baseflow drought based on catchment response times, Hydrology and Earth System Sciences, 22, 6209–6224, https://doi.org/10.5194/hess-22-6209-2018, 2018.

Houben, T.: timohouben/AquiPy: HESS-v0.1, https://doi.org/10.5281/ZENODO.17610247, 2025a.

Houben, T.: Data accompanying the manuscript: Spectral Analysis of Groundwater Level Time Series for Robust Estimation of Aquifer Response Times, https://doi.org/10.5281/ZENODO.17610314, 2025b.

https://doi.org/10.5194/egusphere-2025-5666
Preprint. Discussion started: 20 November 2025

Houben, T., Pujades, E., Kalbacher, T., Dietrich, P., and Attinger, S.: From Dynamic Groundwater Level Measurements to Regional Aquifer Parameters— Assessing the Power of Spectral Analysis, Water Resources Research, 58, https://doi.org/10.1029/2021wr031289, 2022.

IPCC: Climate Change 2022 – Impacts, Adaptation and Vulnerability: Working Group II Contribution to the Sixth Assessment Report of the Intergovernmental Panel on Climate Change, Cambridge University Press, ISBN 9781009325844, https://doi.org/10.1017/9781009325844, 2023.

Jasechko, S., Seybold, H., Perrone, D., Fan, Y., Shamsudduha, M., Taylor, R. G., Fallatah, O., and Kirchner, J. W.: Rapid groundwater decline and some cases of recovery in aquifers globally, Nature, 625, 715–721, https://doi.org/10.1038/s41586-023-06879-8, 2024.

Jazaei, F.: Toward Improved Understanding of Aquifer Response Time Scales, Ph.D. thesis, Faculty of Auburn University, 2017.

Jiménez-Martínez, J., Longuevergne, L., Le Borgne, T., Davy, P., Russian, A., and Bour, O.: Temporal and spatial scaling of hydraulic response to recharge in fractured aquifers: Insights from a frequency domain analysis, Water Resources Research, 49, 3007–3023, https://doi.org/10.1002/wrcr.20260, 2013.

Kumar, R., Samaniego, L., and Attinger, S.: Implications of distributed hydrologic model parameterization on water fluxes at multiple scales and locations, Water Resources Research, 49, 360–379, https://doi.org/10.1029/2012wr012195, 2013.

Kumar, R., Musuuza, J. L., Van Loon, A. F., Teuling, A. J., Barthel, R., Ten Broek, J., Mai, J., Samaniego, L., and Attinger, S.: Multiscale evaluation of the Standardized Precipitation Index as a groundwater drought indicator, Hydrology and Earth System Sciences, 20, 1117–1131, https://doi.org/10.5194/hess-20-1117-2016, 2016.

Kumar, R., Samaniego, L., Thober, S., Rakovec, O., Marx, A., Wanders, N., Pan, M., Hesse, F., and Attinger, S.: Multi-Model Assessment of Groundwater Recharge Across Europe Under Warming Climate, Earth's Future, 13, https://doi.org/10.1029/2024ef005020, 2025.

Lee, S. and Ajami, H.: Comprehensive assessment of baseflow responses to long-term meteorological droughts across the United States, Journal of Hydrology, 626, 130 256, https://doi.org/10.1016/j.jhydrol.2023.130256, 2023.

Liang, X. and Zhang, Y.-K.: Temporal and spatial variation and scaling of groundwater levels in a bounded unconfined aquifer, Journal of Hydrology, 479, 139–145, https://doi.org/10.1016/j.jhydrol.2012.11.044, 2013.

Liang, X. and Zhang, Y.-K.: Analyses of uncertainties and scaling of groundwater level fluctuations, Hydrology and Earth System Sciences, 19, 2971–2979, https://doi.org/10.5194/hess-19-2971-2015, 2015.

Marx, A., Boeing, F., Rakovec, O., Müller, S., Özge Can, Malla, C., Peichl, M., and Samaniego, L.: Auswirkungen des Klimawandels auf Wasserbedarf und -dargebot, Wasserwirtschaft, 2021.

OpenTopography: Shuttle Radar Topography Mission (SRTM) Global, https://doi.org/10.5069/G9445JDF, 2013.

Pujades, E., Kumar, R., Houben, T., Jing, M., Rakovec, O., Kalbacher, T., and Attinger, S.: Towards the construction of representative regional hydro(geo)logical numerical models: Modelling the upper Danube basin as a starting point, Frontiers in Earth Science, 11, https://doi.org/10.3389/feart.2023.1061420, 2023.

Samaniego, L., Kumar, R., and Attinger, S.: Multiscale parameter regionalization of a grid-based hydrologic model at the mesoscale, Water Resources Research, 46, https://doi.org/10.1029/2008wr007327, 2010.

Samaniego, L., Thober, S., Kumar, R., Wanders, N., Rakovec, O., Pan, M., Zink, M., Sheffield, J., Wood, E. F., and Marx, A.: Anthropogenic warming exacerbates European soil moisture droughts, Nature Climate Change, 8, 421–426, https://doi.org/10.1038/s41558-018-0138-5, 2018.

Schilling, K. E. and Zhang, Y.-K.: Temporal Scaling of Groundwater Level Fluctuations Near a Stream, Ground Water, 50, 59–67, https://doi.org/10.1111/j.1745-6584.2011.00804.x, 2011.

https://doi.org/10.5194/egusphere-2025-5666
Preprint. Discussion started: 20 November 2025

Wanders, N. and Wada, Y.: Human and climate impacts on the 21st century hydrological drought, Journal of Hydrology, 526, 208–220, https://doi.org/10.1016/j.jhydrol.2014.10.047, 2015.

Welch: The use of the fast Fourier transform for the estimation of power spectra: A method based on time averaging over short, modified periodograms, IEEE Trans. Audio Electroacoust, 15, 70–73, 1967.

Woessner, W. W.: Groundwater-Surface Water Exchange, The Groundwater Project, https://books.gw-project.org/groundwater-surface-water-exchange/chapter/perennial-intermittent-and-ephemeral-streams/, 2020.

Zhang, X., Li, H., J., J. J., Luo, X., Kuang, X., Mao, R., and Hu, W.: Fractal Behaviors of Hydraulic Head and Surface Runoff of the Nested Groundwater Flow Systems in Response to Rainfall Fluctuations, Geophysical Research Letters, 49, https://doi.org/10.1029/2021gl093784, 2022.

Zhang, Y.-K. and Li, Z.: Effect of temporally correlated recharge on fluctuations of groundwater levels, Water Resources Research, 42, https://doi.org/10.1029/2005wr004828, 2006.

Zhang, Y.-K. and Schilling, K.: Temporal scaling of hydraulic head and river base flow and its implication for groundwater recharge, Water Resources Research, 40, https://doi.org/10.1029/2003wr002094, 2004.

Zhang, Y.-K. and Schilling, K.: Temporal variations and scaling of streamflow and baseflow and their nitrate-nitrogen concentrations and loads, Advances in Water Resources, 28, 701–710, https://doi.org/10.1016/j.advwatres.2004.12.014, 2005.

Zhang, Y.-K. and Yang, X.: Effects of variations of river stage and hydraulic conductivity on temporal scaling of groundwater levels: numerical simulations, Stochastic Environmental Research and Risk Assessment, 24, 1043–1052, https://doi.org/10.1007/s00477-010-0437-5, 2010.

Zink, M., Kumar, R., Cuntz, M., and Samaniego, L.: A high-resolution dataset of water fluxes and states for Germany accounting for parametric uncertainty, Hydrology and Earth System Sciences, 21, 1769–1790, https://doi.org/10.5194/hess-21-1769-2017, 2017.